Magnetotactic Bacteria

International Edition: DOI: 10.1002/anie.201408900
German Edition: DOI: 10.1002/ange.201408900

From Bacteria to Mollusks: The Principles Underlying the Biomineralization of Iron Oxide Materials

Damien Faivre and Tina Ukmar Godec*

Keywords:
biomineralization · goethite · iron · magnetite · magnetotactic bacteria

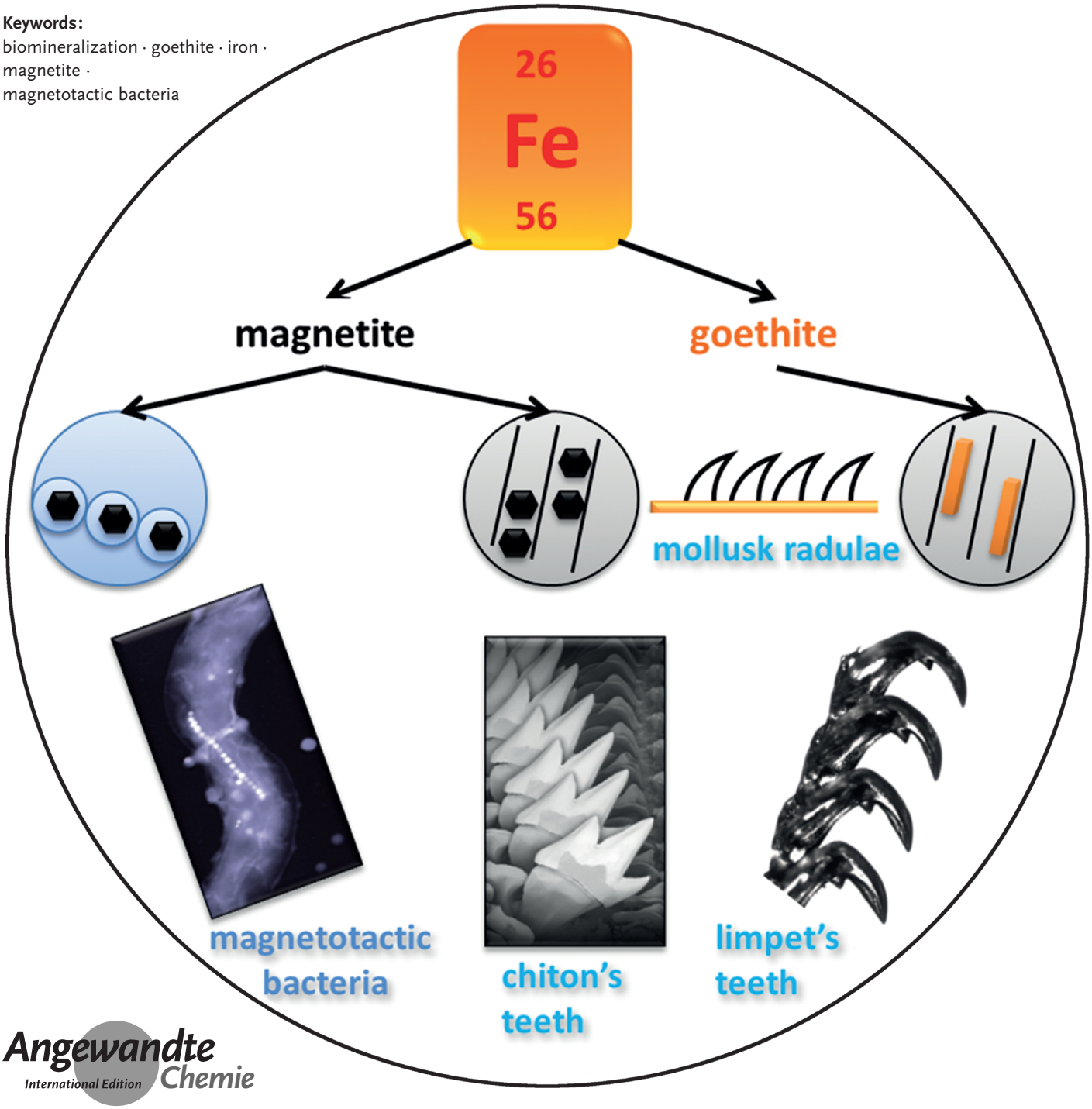

Various organisms possess a genetic program that enables the controlled formation of a mineral, a process termed biomineralization. The variety of biological material architectures is mind-boggling and arises from the ability of organisms to exert control over crystal nucleation and growth. The structure and composition of biominerals equip biomineralizing organisms with properties and functionalities that abiotically formed materials, made of the same mineral, usually lack. Therefore, elucidating the mechanisms underlying biomineralization and morphogenesis is of interdisciplinary interest to extract design principles that will enable the biomimetic formation of functional materials with similar capabilities. Herein, we summarize what is known about iron oxides formed by bacteria and mollusks for their magnetic and mechanical properties. We describe the chemical and biological machineries that are involved in controlling mineral precipitation and organization and show how these organisms are able to form highly complex structures under physiological conditions.

From the Contents

1. Introduction

1.1. Biomineralization

Biomineralization is typically the formation, by organisms, of purely inorganic or composite (inorganic–organic mixture) materials named biominerals. There is a large variety of biomineral types and associated organisms, which was recognized very early by mankind, who used biological materials as tools. The discovery of the full diversity of biominerals only came with the development of microscopic and analytical tools, and at the end of the 19th century, in the work of Haeckel,[1] an extensive list could be generated. A more modern list appeared about a century later in the seminal work of Lowenstam.[2] The list of biomineral classes includes sulfates, carbonates, phosphates, oxides, hydroxides, and sulfides, to name a few. Skinner presented a long list of biominerals and the reader who is interested in the variety of biominerals is referred to her Review.[3] The types of organisms that form these biominerals can be found, for example, in the book by Lowenstam and Weiner,[4] even if further biomineralizing organisms have been studied in the meantime.

The term biomineralization is not limited to the formation of hard matter in the solid-state and the mixing of inorganics with organics to achieve properties otherwise unattainable with a pure mineral phase. In other words, biomineralization also encompasses how the organisms structure their mineral inclusions to obtain a function that otherwise would not have been possible by simply controlling the physics and chemistry of the transport and deposition of elements. Recent research in the field has concentrated on how these biological materials are structured, with a specific emphasis on the hierarchical organization and its role on function.[5] In addition, biologists are searching for biological determinants, typically genes and proteins that are responsible for the controlled deposition of the biomaterials and the associated materials properties.

A striking point from a mineralogical point of view is that in biomineralization the organisms are not limited to controlling the mineral nature based on given elements. A given polymorph can be selectively formed by biomineralization even if it is thermodynamically less stable than another. A typical example is the formation of vaterite or aragonite in certain mussel shells instead of thermodynamically more stable calcite.[6] In addition, biological organisms can tune the morphology of their mineral in a way that defies crystallographic symmetries. For example, magnetotactic bacteria form elongated crystals of magnetite, a spinel mineral that is known to crystallize in a cubic system for which anisotropic crystals are not expected.[7] The terminology "biomineral" also encompasses particulate matter with only short-range ordering, such as silica formed by diatoms.

Biomineralization is intrinsically interdisciplinary since it links the living world of organisms and their soft, mostly organic tissues with the inanimate geological world of rocks and their hard, mostly inorganic materials.[8] Biomineralization is a large source of inspiration for chemists, materials scientists, and engineers, who can learn how to form functional materials with a restricted amount of chemical elements and at environmental and/or physiological condi-

[*] Dr. D. Faivre, Dr. T. U. Godec
Max-Planck-Institut für Kolloid- und Grenzflächenforschung
Wissenschaftspark Golm
14424 Potsdam (Germany)
E-mail: damien.faivre@mpikg.mpg.de
Homepage: http://www.mpikg.mpg.de/135282/MBMB
Dr. T. U. Godec
National Institute of Chemistry
Hajdrihova 19, 1000 Ljubljana (Slovenia)

Supporting information for this article is available on the WWW under http://dx.doi.org/10.1002/anie.201408900.

tions.[5b,9] The elucidation of the structure–function relationship in biological materials allows design principles to be extracted that in turn can be used as novel concepts in materials science and engineering.[5]

The literature on in situ experiments involving mineral deposition in the presence of proteins, polymers, and at various surfaces is abundant for calcium minerals (see for example Ref. [9d]). However, iron is one of the most abundant elements in the Earth's crust and it has long been and still is the basis of several materials formed by humans. Steel as an example of iron-based materials is typically formed at very high temperature. Alternatively, iron oxide biominerals are form under green conditions without loss of functionalities so that they have potential for numerous scientific as well as industrial applications[10] and therefore there is much to learn from biomineralization in the field. Herein, we will thus focus on iron oxide biomineralization (magnetite and goethite) and will specifically present their formation by organisms from different kingdoms (magnetotactic bacteria, chitons, limpets).

1.2. The Different Types of Biomineralization

Biomineralization, as is the case with many other scientific areas, has been separated into subdisciplines highlighting the diversity of the field. This was, for example, performed on the basis of the different processes leading to biominerals. In this case, the biological minerals are either the result of a biologically induced or a biologically controlled process.[8e] The biologically induced process is typically the result of an extracellular mineralization originating from a passive cellular mechanism, such as respiration. This type of biomineralization is not directly genetically controlled, since even if the organism influences its direct environment in which the mineral is formed, it cannot extensively control the mineral properties, since biomineralization happens in a widely open system. Mineralization is therefore often observed at the surface of cells, which serves as the origin of heterogeneous nucleation. As a result, the particle size distribution is broad and no dedicated particle morphology is observed.[11]

In contrast, in biologically controlled mineralization, the nucleation, growth, morphology, and final location of the biomineral is genetically controlled. Mineralization can occur extra-, inter-, or intracellularly.[8e] The biominerals we are presenting in this Review all fall within this category. The highest degree of control can be obtained for intracellular biomineralization, which is typical for microorganisms. In intracellular mineralization, the cells form the mineral intracellularly inside dedicated organelles, even if the mineral can be transported extracellularly at a later stage, for example, to the cell surface.

In this Review, we will start by presenting the general framework of biomineralization. We will show that several steps occur before the mineral can be deposited in its final destination. We will detail the current knowledge about the structure and the chemical mechanistic pathways leading to the respective formation of magnetite by magnetotactic bacteria and chitons, and of goethite by limpets. We will present what is known about the biological determinants involved in the formation and organization of the different minerals. Later, we will show that the magnetotactic bacteria represent a model organism of choice for biomineralization since genetic tools are available for the generation of knockout mutants, which allows the precise molecular roles played by individual biological determinants to be elucidated. Such a possibility is currently lacking in other organisms and therefore much less is known at the molecular level. We will finish by presenting a brief summary and outlook for possible research in the multidisciplinary field of iron oxide biomineralization.

2. General stages of biomineralization

From the chemical point of view, there is no reason to differentiate between typical chemical or geological mineralization and biomineralization pathways. Both mineralization processes should follow classical nucleation rules. Thus, in order to form a mineral, the organisms have to take up a given element or a combination of elements from the environment. These elements are possibly found in the form of ions or complexes and transported intracellularly by active biologically driven processes or simple passive diffusion. Once the inner part of the cell is reached, the elements will be concentrated and eventually nucleated. An additional transport step within the organism may be possible. These different steps are described below in a general framework.

Following the rules of classical nucleation, crystal formation requires the accumulation of a supersaturated concentration of a solute. In fact, from classical nucleation theory, a critical nucleus will be formed, when the concentration of

Damien Faivre studied physical chemistry at the Claude Bernard University (Lyon, France) and at Concordia University (Montreal, Canada). His doctoral thesis in geochemistry was performed at the Institute for Earth Physics (Paris, France) and the California Institute of Technology (Pasadena, USA); before joining in 2005 the group of D. Schüler as a Marie Curie Fellow at the Max Planck Institute of Marine Microbiology (Bremen, Germany). He moved to Potsdam in 2007 as group leader. He was awarded a starting grant from the ERC in 2010.

Tina Ukmar Godec studied pharmaceutical science at the University of Ljubljana (Slovenia) and obtained her masters in materials chemistry in 2008. She completed her doctoral thesis in the area of physical chemistry at the National Institute of Chemistry, Ljubljana, Slovenia and obtained her Ph.D. in Biomedicine from the University of Ljubljana in 2011. After maternity leave she joined the group of Damien Faivre as a postdoctoral researcher at the Max Planck Institute of Colloids and Interfaces in 2014.

a dissolved constituent exceeds the equilibrium solubility. This supersaturation allows for the assembly of molecules or atoms in a stable ordered crystalline form (see example Ref. [12]). So-called non-classical pathways have also been proposed for biomineral formation, where precursor phases are based on poorly crystalline materials.[13] These precursors may lower the energetic step leading to the formation of the final crystalline material.[14]

In both possible mechanisms, the formation of a crystal requires the uptake of a large quantity of the elements building up the structure of the biomineral. In the specific case of iron, this task is particularly difficult since iron is a poorly soluble element. Therefore, particular mechanisms might be required, as we will see in Section 3 in the case of the magnetotactic bacteria. The mechanism of this uptake, to our knowledge, has indeed not been fully clarified in multicellular organisms. Model unicellular organisms are critical in the study of biomineralization, since more can be learned from them, because their genomes are sequenced and genetic tools are available for the modification of their pool of genes. Ion uptake can be genetically controlled by ion transporters, or ion pumps, or some ion channels, which may enable the facilitated passive diffusion of ions through biological barriers (i.e., membranes).

The elements required for mineralization might enter the cell directly at the site where they will be mineralized. Alternatively, once the elements have entered the cell, they might be transported towards the intracellular deposition site. If further transport is needed, since the biominerals are typically deposited within dedicated organelles with their own protein systems, similar ion pumps and channels used for the cellular uptake might be at work. A chemical or structural modification of the iron species of interest, after entering the cell, is probable and is often observed, specifically in the case of temporary storage. A typical storage protein complexing iron is ferritin. The formation of ferritin and its properties are, however, outside the scope of this work and the interested reader is referred to the work of Arosio et al.[15]

Once the elements are transported to their deposition site, they need to be transformed into the biomineral of interest. Since intracellular biomineralization usually happens in microorganisms in dedicated compartments, the physico-chemical parameters required for nucleation and growth may be adjusted, for example, by the use of proton-translocation systems for the adjustment of the pH value, or by redox-active proteins, such as cytochrome, for the adjustment of the redox potential. This adjustment is less clear in the case of higher organisms. We will see in the following Sections, which biological macromolecules are involved in the process of biomineralization for the three model organisms of interest.

3. Formation of Magnetic Nanostructures by Magnetotactic Bacteria

3.1. Magnetotactic Bacteria

"Magnetosensitive" bacteria were first discovered in the 1960s, however, Bellini's reports were only recently translated from the Italian and published.[16] Thus, it is Blakemore's finding of magnetotactic bacteria, about 40 years ago, that can be considered as the first report of iron biomineralizing microorganisms.[17] At the time, a group of bacteria were discovered that swam constantly in the same geographical direction.[17] Placing a magnet in the vicinity of the sample, collected near Woods Hole in Massachusetts (USA), altered the swimming direction of the cells, a process Blakemore called magnetotaxis. This behavior is due to the presence of magnetic nanoparticles aligned in a chain within the body of the cells. The particles are embedded in membranes and the assemblage particle-membrane is called a magnetosome.

Since their discovery magnetotactic bacteria have attracted interest from diverse scientific disciplines ranging from the biological sciences, such as microbiology, cell biology, and biotechnology, to Earth and planetary sciences, physics, and chemistry. The cells in fact were used in the definition of biogenicity criteria in the late 1990s.[18] More recently, the bacteria have become a model system for the study of biomineralization since the genomes of several strains are sequenced and since genetic tools are available to manipulate their genes.[19] Moreover, and with the advancement of bio- and nanotechnologies, their magnetosomes have been shown to have potential biomedical applications.[20] This group of bacteria is also of particular interest for chemists and materials scientists, since they excel where humans are still stumbling: the self-assembly of nanoscale building blocks. The synthesis of bacterial magnetosome chains requires highly regulated mechanisms to control first the formation of the magnetosome membrane resulting in empty vesicles; second the iron uptake and transport from the environment to the organelle; third the biomineralization of the magnetic nanoparticles with controlled size and morphology; and finally the organization of the magnetosomes into an ordered nanostructure.

Magnetotactic bacteria[17] are a group of microorganisms (see Table 1 in the Supporting Information) that synthesize and organize magnetic nanoparticles called magnetosomes. Magnetotactic bacteria are Gram-negative bacteria which are very diverse in terms of, for example, cellular morphology, environmental origin, physiological needs, and phylogeny.[21] As examples, spirilla-, vibrio-, or rod-shaped bacteria have been identified together with cocci.[21] They live in freshwater, marine, or hypersaline environments and belong to the Alpha-, Gamma-, and deltaproteobacteria class of the Proteobacteria phylum as well as to the Nitrospirae phylum and the candidate division OP3.[21] Even the flagellar systems responsible for the bacterial motility differ: some cells possess a single polar flagellum, others have one flagellum at each cell pole or a bundle of flagella at a given pole (Figure 1). To date, no relationship was observed between the flagellar system, the cellular morphology, and the preferred environment or the classification.

The magnetosomes[22] are membrane-enveloped magnetite (Fe_3O_4) or greigite (Fe_3S_4) nanoparticles. In the case of magnetite magnetosomes, the crystals exhibit the perfect structure of the mineral with no deviation towards the oxidized form maghemite, the cell prevents the particles from oxidation.[5d] The dimensions, morphology, and organ-

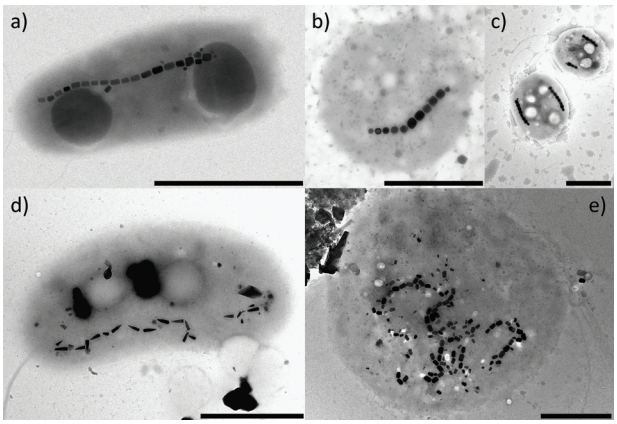

Figure 1. transmission electron microscopy images of magnetotactic bacteria (scale bars are 1 μm, image courtesy of C. Lefèvre). a),b) are cultured strains, strain SS-5 (a) and strain PR-3 (b), both forming elongated particles. c)–e) are naturally occurring bacteria with unusual traits: c) Magnetococci with two chains of magnetosomes (from the Mediterranean sea in Marseille, France), d) a Magnetovibrio forming bullet-shaped magnetosomes running in opposite directions (from a freshwater environment in Camargue, France) and e) a Magnetococcus with non-organized magnetosomes (from the Mediterranean Sea in Sainte Maxime, France).

ization of the crystals are strain-specific (Figure 1) and genetically controlled. The magnetosome dimensions are constant for one strain, but differ between different strains (ranging from about 35 to about 80 nm (Figure 1)).[23] The morphology is also constant for a given strain and morphologies of magnetite crystals, such as the isometric cuboctahedral or the elongated bullet-shaped, have been observed (Figure 1).[23a,24] The size and morphology is such that crystals always form as a so-called stable single magnetic domains, therefore each particle acts as permanent magnet.[25]

The magnetosomes are arranged by the cells to form, typically, a chain, even if multiple chains are also observed in some non-cultured bacteria (Figure 1). The particles in the chain are all aligned along the easy axis of magnetization, which typically corresponds to the cellular long axis.[26] The typical nanometer-scale subcellular structure formed by the assembly of several magnetosome particles in a row is supposedly used by the bacteria as an actuating tool to passively align itself along the Earth's magnetic field lines.[17,27] The current hypothesis is that magnetotaxis facilitates the search for the microaerobic environments, which are preferred by the cells.[27a,b] Thus, a magnetotactic bacterium has been depicted as a "self-propelled magnetic compass needle".[28]

In the following, we will thus first describe the recent advancement in the study of the chemical pathway leading to magnetite nucleation and growth. We will then present the genes and proteins involved in the magnetosome formation and organization, before presenting a model summarizing the current knowledge of bacterial control of size, morphology, and organization of magnetosomes. Then, in Section 3.5 we will present our subjective view of open questions and future challenges in the field.

3.2. Chemical Pathway of Magnetic Particle Formation

Magnetotactic bacteria form either the iron oxide magnetite $Fe^{II}Fe^{III}{}_2O_4$[29] or the iron sulfide greigite $Fe^{II}Fe^{III}{}_2S_4$.[30] Some cells are also able to form both.[31] Most of the mechanistic studies on iron biomineralization were performed on magnetite-mineralizing cells because greigite-mineralizing strains were not available in pure culture until very recently.[31b] Thus, the greigite mineralization pathway is only known from "wild" samples. However, it is currently not known how wide-spread the strain is.[32]

As already above and for the case of all biomineralizing microorganisms, the cells have to take up the elements necessary for mineral formation from their surroundings. In the case of magnetite, it was shown that oxygen originates from the water.[33] The iron in turn can be taken up as Fe^{II} or Fe^{III} iron compounds[19d,34] (Figure 2). Nothing is known about the uptake of elements for greigite formation.

The iron then crosses the outer membrane and enters the cells where different scenarios and precursors have been proposed for magnetite formation in Magnetospirilla strains. Mechanisms involving the presence of ferrihydrite-like materials, of hematite, or of high-spin Fe^{II} complexes have been proposed, with these species localization in the cell or directly inside the magnetosomes.[29,34,35] Recently, a consensus over the mechanism has emerged, thanks to integrated approaches involving magnetic measurements, elemental analysis, X-ray absorption spectroscopy, and high resolution TEM[13d,36] (Figure 2). In this pathway, magnetite forms through phase transformation from a highly disordered phosphate-rich iron(III) hydroxide phase, consistent with prokaryotic ferri-

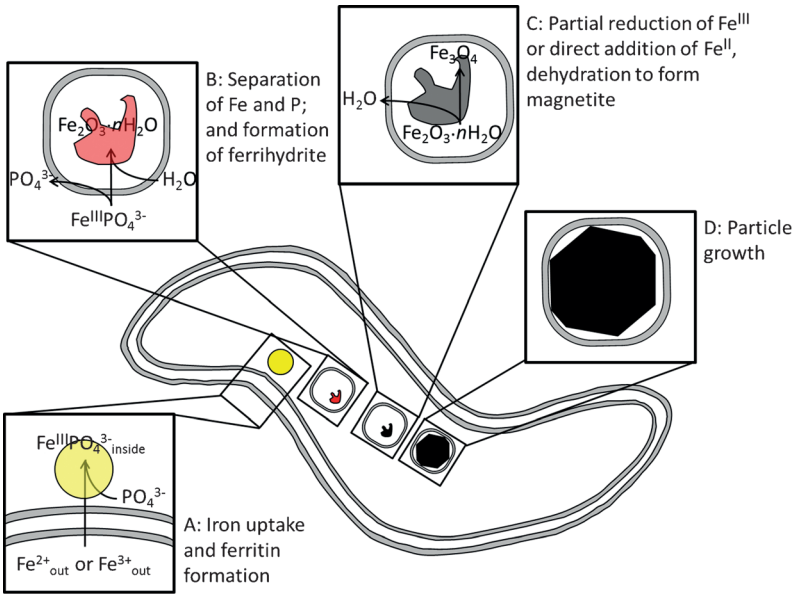

Figure 2. Potential reaction pathway leading to magnetite biomineralization in magnetotactic bacteria (see text for explanation and details).

tins, via transient nanometric iron(III) oxyhydroxide intermediates. In particular, Baumgartner et al.[13d] showed that the ferritin-like precursor (ferrihydrite embedded in the ferritin protein) was localized outside the magnetosome vesicle whereas the ferrihydrite-like intermediate (purely inorganic material) was found inside. Fdez-Gubieda et al.[36] showed that the ferritin-like material was a precursor phase involved in the magnetite formation pathway and not a separate source of iron only used for biochemical purposes. Finally, the presence of hematite could be ruled out and its previous detection was suggested to be associated with the evolution of ferritin-like material under the electron beam.[37] In *Desulfovibri magneticus* RS-1, an iron- and phosphorus-rich organelle, distinct from the magnetite magnetosome, was found.[38] This organelle is not only physically separated from the magnetosomes, but nano-SIMS also showed that the additional organelle was not used as an iron source for magnetite formation.[38] The function of this organelle has thus remained obscure.

The greigite formation process was only studied in bacteria that are not available in pure cultures.[32] Their electron-microscopy analyses demonstrate that greigite forms from mackinawite (tetragonal FeS). The transformation is very slow (10 days), especially when compared to the timescale for magnetite biomineralization (a few hours, maximum).[34,35b,36,39] However, it is not clear if the mechanism proposed by Posfai et al. is relevant for all bacterial strains forming greigite or not. Thus, studies on greigite mineralization in magnetotactic bacteria will profit from the greigite-(and magnetite)-synthesizing organism BW-1 recently isolated in pure culture[31b] which should aid studies especially into mechanistic aspects of iron sulfide mineralization.

3.3. Biological Components Functionally Involved in Magnetosome Formation and Organization

3.3.1. The Magnetosome Membrane

The magnetosome is an intracellular organelle, which consists of a lipid bilayer surrounding the magnetic nanoparticle. The magnetosome membrane is about 3–4 nm thick,[22] and contains a set of phospholipids typical of the inner membrane but distinct from the outer membrane, showing that the magnetosome membrane possibly originates from the inner membrane. In addition, the magnetosome membrane possesses a specific and unique set of proteins very distinct from that of other subcellular compartments.[19b,40] Images of *Magnetospirillum* species by electron cryotomography confirmed that the magnetosomes are invaginations of the inner cell membrane.[41]

3.3.2. The Magnetosome Gene Island

The analysis of isolated magnetosomes led to the identifications of magnetosome-membrane-specific genes. These genes and proteins, responsible for biomineralization, are clustered within the so-called magnetosome island (MAI).[42] It was observed that non-magnetotactic mutants frequently spontaneously form from wild-type cells. This loss of the magnetic phenotype, for example in *Magnetosprillum gryphiswaldense*, is characterized by the loss of a large chromosomal region, the MAI.[43] The magnetosome island basically contains the genes necessary for biomineralization.[44] With the advancement of sequencing techniques, similar genomic regions were found in other magnetotactic strains,[21,45] including greigite-mineralizing strains.[31b,46] In addition, a "mini-MAI" was shown to be sufficient for magnetite mineralization in MSR-1[47] and AMB-1.[48]

The MAI is mainly organized around four gene clusters in *Magnetospirillum gryphiswaldense*, which are the *mms6*, *mamAB*, *mamGFDC*, and *mamXY* operons that encode all known magnetosome membrane proteins. However, they are not all present in every strain. Magnetosome membrane proteins have been named Mam (*ma*gnetosome *m*embrane), Mme (*m*agnetosome *me*mbrane), Mms (*m*agnetic particle *m*embrane *s*pecific), Mtx (*m*agneto*tax*is), or Mad (*ma*gneto-*d*eltaproteobacteria specific). The identified magnetosome membrane proteins display homology with characteristic protein families, which include *t*etratrico*pe*ptide *r*epeat (TPR) proteins (MamA), *c*ation *d*iffusion *f*acilitator (CDF) family of transporters (MamB and MamM), HtrA-like serine proteases (MamE, MamP, MamO), actin-like proteins (MamK), generic transporters (MamH, MamN), and proteins without homology with other known proteins (MamC and MamD).[49] The role of these genes/proteins is explained in the following, when known.

3.3.3. The Magnetosome Organelle

The *mamAB* operon is the only one which is indispensable for magnetic particle production, as the deletion of this cluster in the strains *Magnestoprillum magneticum* (AMB-1)[19a] and in *Magnetospirillum gryphiswaldense* (MSR-1) causes the total loss of the magnetic particles.[47,50] In turn, its expression alone in a complete MAI deletion mutant[47] or in a host organism[51] enables the formation of electron-dense particles. Complementation with other genes eventually enables the formation of magnetosome-like particles.[51]

The individual deletion of any of *mamI*, *mamL*, *mamQ*, and *mamB* results in the disappearance of the magnetosome membrane in AMB-1[19a] with the same effect for *mamB* in MSR-1.[52] MamI and MamL are two small proteins only present in magnetotactic bacteria without homology with any other known proteins. MamL has a 15 amino acid C-terminal, tail rich in positively charged amino acids, which possibly interact with the cytoplasmic side of the inner membrane to create an asymmetry that may trigger the bending of the magnetosome membrane to form the magnetosome organelle (Figure 3).[53] MamQ and MamB have coiled–coil repeat domains that may help to shape the magnetosome membrane.[19a] However, these proteins could have an additional or complementary role, such as the maintenance of the magnetosome membrane shape, once it is already formed, rather than the formation of the vesicle itself.[53] These four proteins are essential, but not sufficient, for the biogenesis of the magnetosome membrane on their own. Indeed, when these genes are restored in a strain lacking the rest of the mamAB gene cluster, no magnetosome membrane formation is

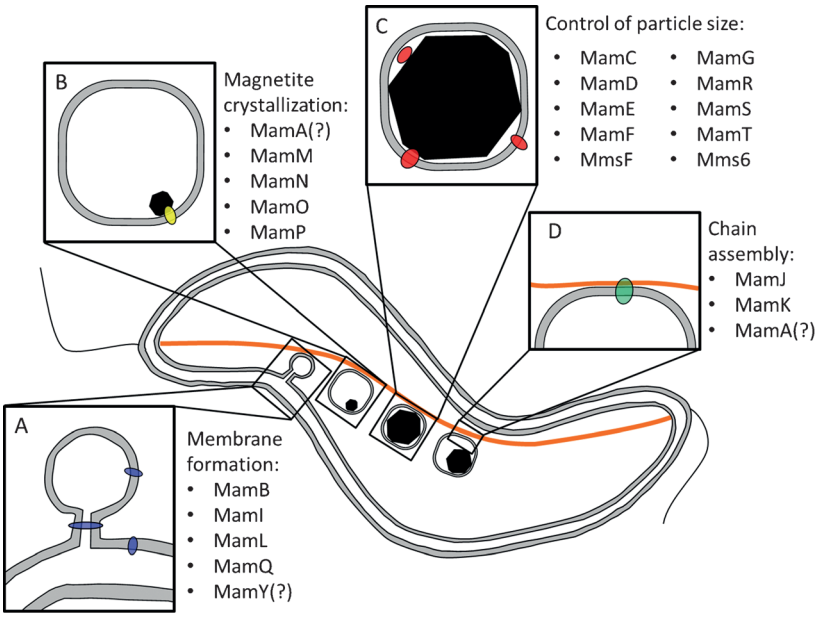

Figure 3. Summary of the proteins potentially involved in the different phases of magnetosome formation and assembly. A) Magnetosome membrane formation: MamB, MamI, MamL,and MamQ, MamY(?) (in blue) could be used to shape and close the vesicle, as well as to sort further proteins. B) Crystallization of magnetite: MamA(?), MamM, MamN, MamO (in yellow). C) Particle size control: MamC, MamD, MamE, MamF, MamG, MamP, MamR, MamS, MamT. D) Chain assembly: MamJ, (anchor proteins in green), MamK (filament proteins in orange), MamA(?) (see text for details and discussion).

observed.[19a] The exact mechanism by which these effects occur has been not clarified.

3.3.4. The Iron Machinery

As explained in Section 2, iron has to be transported across several membranes in order to reach its final deposition site. Since up to about 2% dry weight iron can be found in the magnetotactic bacteria (for comparison, *E. coli* has 0.02% dry weight iron),[19d] the cells have to have a very effective transport system. In non-magnetotactic microorganisms, the iron homeostasis can typically be performed by the use of siderophores,[54] but no conclusive experiments confirm their presence in magnetotactic bacteria.[19d,55]

At the molecular level, the first genes involved in the process have been recently identified. Surprisingly, a non-magnetotactic bacteria-specific system was first identified. It involves a *fur*-like gene, which inhibits magnetosome formation in the MSR-1 strain, however there is no clear mechanistic insight as to how and why this happens.[56] Later studies have shown that *Fur* is used by the cells as a regulator. Indeed, in mutant lacking the *fur* gene, numerous proteins showed an altered expression when compared to the wild type.[57] The *mamAB* gene cluster encodes two important CDF-like proteins putatively involved in the iron machinery: MamM and MamB (Figure 3). These proteins are highly conserved in all magnetotactic bacteria. Site-directed mutagenesis showed that a single amino acid mutation in the sequence in MamM causes the formation of particles with different shape and size, or aggregates of polycrystalline particles of magnetite or hematite, thus showing that the iron machinery was changed when the genes are modified.[52]

Recently, the role of a redox-controlling protein was investigated. MamP is a c-type cytochrome, also called magnetochrome, exclusively found in magnetotactic bacteria (Figure 3). Δ*mamP* mutants of AMB-1 form less and smaller magnetosomes.[19a,58] MamP acts as an iron oxidase that contributes to the formation of iron(III) ferrihydrite eventually required for magnetite crystallization in vivo. MamX, MamZ, and MamH are also involved in redox control of magnetite biomineralization.[59] In their absence, hematite[59a] or smaller magnetite particles[59b] are formed at the end of magnetosome chains where freshly nucleated magnetosomes are found. These results indicate an impairment of proper biomineralization initiation by a yet unknown mechanism.

3.3.5. The Biological Determinants Controlling Magnetosome Properties

The magnetosome membrane provides the correct bio-physico-chemical environment for triggering crystal formation. The differences in dimensions, shapes, and organizations of magnetosomes seen among the different magnetotactic bacteria suggest that biological determinants are involved in the control of these magnetosome properties. Proteins, such as mamE, mamO, mamM, and mamN, are important players in magnetosome formation in AMB-1[19a] (Figure 3). Knock-out mutants for these proteins are non-magnetic and do not produce electron-dense particles.[19a] Nevertheless, chains of empty magnetosome membranes are still present.[19a,60] This phenotype may be due to a direct involvement of the proteins in the mineral production or to an incorrect localization of the magnetosome proteins. The loss of further MamAB genes, such as *mamP*, *mamT*, *mamS*, and *mamR*, have a less drastic effect because they "only" change the number and the size of crystals produced per cell in the AMB-1 strain.[19a] However, such a phenotype is redundantly (that is, usually) observed in studies involving deletion mutants. MamA in turn, is a protein involved in protein–protein interaction in which its oligomerization may help in the assembly of magnetosome membrane associated proteins.[61] Further investigations are required to quantify and confirm these observations and to explain the mechanism by which they impact biomineralization.

The *mamGFDC* cluster is a region conserved in the MAI of many alpha-proteobacteria, but not in the delta-proteobacteria.[62] It encodes the small hydrophobic MamGFDC proteins, which represent nearly 35% of all proteins associated with the magentosome membrane in *Magnetospirillum gryphiswaldense* MSR-1 cells, but play a non-essential role in biomineralization.[63] MamGFDC proteins plausibly control magnetite growth by changing the physicochemical condi-

tions inside the vesicles, such as the charge distribution at the inner surfaces, or by changing the dimensions of the organelles themselves.[63]

Mms6 is a small acidic protein that is tightly associated with bacterial magnetite in *Magnetospirillum magneticum* AMB-1(Figure 3).[64] It is an amphiphilic protein with an N-terminal hydrophobic region and C-terminal hydrophilic region. Its C-terminal region has been suggested as an iron-binding site.[64] In vivo it has been demonstrated that in AMB-1, deletion of its operon causes smaller and elongated crystals[65] while in MSR-1, 58% of crystals within the cells still had a cubic appearance.[66] More precisely, the small MmsF protein, present in the *mms6* cluster plays a determinant role in the control of magnetosome dimensions and morphology.[48]

Recent studies, investigating the molecular mechanism controlling the crystal morphology, point to the protein Mms6 as playing a role in this control, at least in AMB-1.[65,67] A hydrophobic leucine–glycine repeat motif has been identified in the Mms6 protein and it has been suggested that Mms6 interacts with magnetite and iron ions.[65,68] However, definitive evidence is still lacking. MmsF as well as proteins from the *mamXY* cluster were also shown to be involved in magnetosome morphology control.[47,48,59] However, since synthetic magnetite crystallization typically leads to cubooctahedral crystals,[23a,69] the roles of genes in morphological control of isometric magnetosomes will remain unclear as long as no mechanism is proposed for such a control.

In turn, Lefèvre et al. recently presented a comparative genomic analysis of magnetotactic *Deltaproteobacteria* that synthesize bullet-shaped crystals of magnetite and/or greigite.[146] They found a conserved set of genes, in addition to the *mam* genes. These *mad* genes specific to the magnetotactic Deltaproteobacteria, and in other strains that form bullet-shape magnetosomes, such as in *Candidatus Magnetobacterium bavaricum* of the *Nitrospirae* phylum, are absent in the magnetotactic alphaproteobacteria and therefore constitute a putative base for morphology-controlling genes. Experimental evidence is required to confirm that this is the case.

3.3.6. The Magnetosome Filament and the Magnetosome Connector Involved in Magnetosome-Chain Assembly

Magnetosomes are arranged in single or multiple chains. Within single chains, the cellular magnetic dipole is the sum of the permanent magnetic dipole moments of the individual magnetosomes.[70] Unaided by additional structures, a row of magnetic dipoles should collapse upon itself to lower its magnetostatic energy.[71] The magnetosome filament, therefore, gives mechanical stability to the magnetosome chain and prevents this collapse.[72] Two complementary cryoelectron tomography studies showed the presence of filament bundles. Individual filaments, 3–4 nm in diameter, traverse the cells.[73] Magnetosomes are attached to this magnetosome filament (MF), at least partly formed by the MamK protein,[73b,74] by the magnetosome connector MamJ[73a] (Figure 3). The *mamJ* and *mamK* genes are located within the *mamAB* gene cluster in Magnetospirillum species and are co-transcribed.[75]

MamK has homology to the cytoskeletal actin-like MreB protein that forms cytoskeletal structures in some non-magnetotactic bacteria and is involved in a number of essential cellular processes in bacteria, such as cell-shape determination, establishment of cell polarity, and chromosome segregation.[76] However, MamK proteins in magnetotactic bacteria are more similar to each other than they are to MreB homologues.[73b,77] The magnetosome filament was not imaged in a mutant of AMB-1 from which the *mamK* gene was deleted[73b] even though a second version of the gene is present in the genome.[78] AMB-1 MamK forms straight filaments rather than helical structures.[79] MamK presumably has a more complex function than just providing a rigid scaffold for magnetosome alignment as it could also play a role in positioning and concatenating magnetosome chains.[80] This protein also has an important function in splitting magnetosome chains during cytokinesis and its presence is required for proper magnetosome position and segregation.[80] The *ftsZ*-like gene of MSR-1, a cousin of *mamK*, is surprisingly not directly involved in magnetosome structuring, but rather, as for most of other genes for which the function is unclear, in the control of magnetosome dimension and magnetosome number.[81]

The MamJ protein is an acidic protein with a repeating glutamate-rich section in its central domain.[82] The *mamJ* gene immediately precedes *mamK* within the *mamAB* operon. The MamJ protein interacts with the MamK filament and directs the assembly and localization of the prokaryotic organelles along the chain in MSR-1.[82–83] The deletion of the *mamJ* gene causes magnetosomes not to assemble in linear chains but instead to arrange in three-dimensional clusters.[82] In the case of AMB-1 two proteins, MamJ and LimJ, perform a redundant role (that is, if one is absent the other takes over) in promoting the dynamic behavior of MamK filaments in wild-type cells. However, their deletion does not cause the collapse of the magnetosome chain. The absence of both MamJ and LimJ leads to static filaments, a disrupted magnetosome chain, and an anomalous build-up of cytoskeletal filaments between magnetosomes.[84] MamJ could also potentially retard magnetite formation since such a role has been shown in vitro.[85]

3.4. Nanotechnology: Use of Magnetotactic Bacteria and Applications of Magnetosomes

Owing to their unique magnetic properties, several bio- and nanotechnological applications have been envisioned for magnetosomes and magnetosome chains.[20a,86] The ease of modification of the magnetosomes has been exploited by Matsunaga et al. for the purification, isolation, and detection of mRNA and DNA.[87] Particularly, they observed the superiority of magnetosomes over synthetic magnetic nanoparticles for DNA recovery.[87a] Other applications arise from the functionalization of magnetosome surfaces: chemical approaches are achieved by cross-linking,[87b,88] conjugation of amine-modified oligonucleotides,[87c] immobilization of myosin,[89] and biotynilation.[90] These functionalized magnetosomes can be used for the selective separation of biological/

chemical targets, as analytical probes of chemical environment, and for ultra-sensitive detection. Alternatively, surface functionalization is achieved with genetic tools. This involves the construction of genetic fusions of magnetosome-membrane anchor polypeptides with functional proteins and enzymes.[91] Genetic approaches have the advantage of better preserving the protein activity of magnetosomes, permitting the display and screening of various enzymes, proteins, and compounds,[92] and even the development of new microfluidic assays.[93] Genetic fusion on magnetosomes has also permitted the expression of fluorescent proteins or nanobodies by the bacterial proteins.[94]

The properties conferred by the magnetosome chain on the magnetotactic bacteria permit the control of the bacteria using an externally applied magnetic field and their tracking using magnetic resonance imaging (MRI),[95] which has been envisioned for medical nanorobotic applications. Other possible applications result from the use of magnetosomes as contrast agents for MR imaging.[96] Magnetosomes and magnetosome chains have potential application in hyperthermia. This technique requires magnetic nanoparticles that exhibit high heat production following the reorientation of their magnetic moment. The reorientation is typically induced by an externally applied alternating magnetic field and results in the specific necrosis of tumor cells. Chains of magnetosomes rather than individual magnetic nanoparticles have for more beneficial effect.[97]

3.5. Open Questions

Indirect, mostly in vitro experiments, indicate that physico-chemical parameters dominate within the magnetosome organelle at the time of magnetite formation. For example, the iron concentration[98] as well as the pH value[99] have been indirectly evaluated based on similarities between the synthetic[100] and biological[13d] formation mechanisms. However, direct measurements of pH value, redox potential (E_h), and iron concentration would be very interesting to confirm the hypothesis that mineralization and biomineralization follow similar pathways.

On a more biological side, although the minimal set of genes necessary for magnetite formation has been identified, the minimal set of genes for regulating the magnetite size are not known; the genes controlling the number of magnetosome particles have not been identified, and the genes responsible for magnetosome morphology remain completely unknown, partly because the genetic systems for bacteria with anisotropic morphologies are not yet established. However, this task is hampered by the fact that a single gene is certainly not solely responsible for a given property, instead a protein complex is probably doing the work. Such complexes are of course more difficult to identify, partly because some genes with redundant functions are hidden, even outside the MAI.

4. Biomineralization in Radulae of Marine Mollusks

4.1. Chitons and Limpets

Chitons and limpets form magnetite and goethite, respectively, as materials for the veneer of their radular teeth. The minerals are used as reinforcement materials to improve the mechanical properties of the teeth. Such reinforcement is a successful strategy as the radular teeth of marine mollusks are among the hardest and stiffest known biominerals[101] (e.g. the magnetite layer in the chitons *Chiton olivaceus* and *Acanthopleura gemmata* was found to have a Vickers hardness between 322 and 646 $kg\,m^{-1}\,m^{-2}$ with a mean value of 433 and 537 $kg\,m^{-1}\,m^{-2}$, for *C. olivaceus* and *A. gemmata* respectively).[102] As a comparison, inorganic magnetite (when measured with the same setup and experimental conditions) was measured to have a Vickers hardness between 639 and 701 $kg\,m^{-1}\,m^{-2}$ and a mean value of 676 $kg\,m^{-1}\,m^{2}$. The hardest part of teeth of limpet *Patella vulgata*, was found to be somewhat softer with a hardness between 268 and 602 $kg\,m^{-1}\,m^{-2}$ and a mean value of 413 $kg\,m^{-1}\,m^{-2}$.[102] The radula is a several cm-long tongue-like organ, the last 2–5 mm of which extend out of the mollusk's mouth (see Figure 4a). These organisms use radulae (a rasping, toothed conveyor-belt-like structure used for feeding) to scrape rocks in order to extract algae (Figure 4a). More than 100 rows of teeth are anchored to the radula (Figure 4b–e), where only the outermost 10 rows are used for scraping.[4] A row of teeth is worn down on average every 12–48 h and new teeth are continuously formed at the same time.[103] By radular growth, the teeth advance into position and eventually enter the scraping zone. Finally, after reaching the outermost position, they detach from the rest of the radula. The radula is therefore perfectly suitable for a systematic study of the various stages of biomineralization by a row-by-row analysis since different rows carry teeth at different stages of mineral formation. In addition to a superior hardness, the teeth are designed in such a way as to ensure a well-defined plane of wear at all times, giving rise to a, so-called, self-sharpening effect (Figure 4g).[101,104] Thus, these mollusks could serve as nature's guide towards developing self-sustainable hierarchical functional materials.

Chitons (Mollusca, Polyplacophora) are an ancient, but a relatively small group of mollusks with roughly 750 species inhabiting rocky coastal regions around the world, and are found from intertidal to abyssal zones.[101a,103,106] They are slow moving, flattened, symmetric, elongated, and herbivorous mollusks protected dorsally by eight overlapping shell plates; they graze for algae on hard substrates. In turn, limpets (Mollusca, Gastropoda) are a large group of rather primitive herbivorous marine organisms that also feed on algae from rocks.[107] They typically have cone-shaped shells and are mostly found in the intertidal zone.

In both chitons and limpets newly formed teeth consist of a three-dimensional α-chitin matrix with associated proteins, while mature teeth contain at least one iron and one non-iron biomineral.[108] More detailed structural features are specific to each of the two types of mollusks but the hierarchical and spatially highly organized composite structure is generically

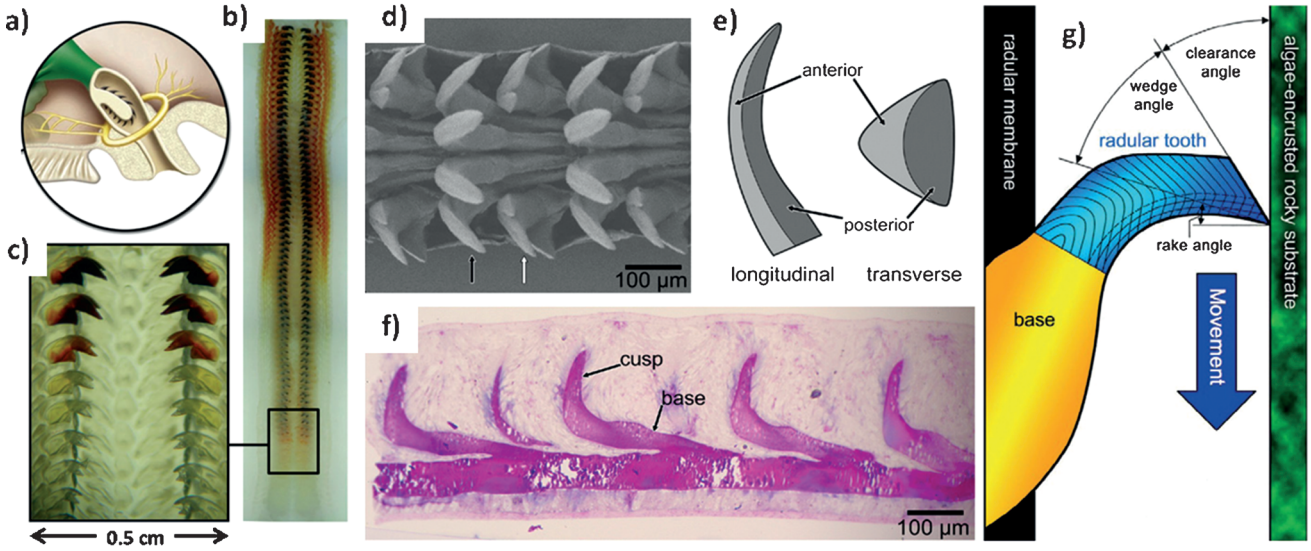

Figure 4. a) Schematic of the chiton *Criptochiton stellari* mouth containing the radula; b) Optical micrograph of the radula of *C. stellari*; c) Magnification of the transitional zone near the posterior end of the radula depicting a gradual change in tooth color from transparent to black, indicating the onset of mineralization; d) SEM micrograph of a part of the radula of limpet *Patella caerulea* with radular sac removed to show the teeth. Six mineralized teeth are present in each row: four unicuspid teeth (black arrow) and two tricuspid teeth (white arrow). e) Schematic representation of the anatomy of a tooth cusp: leading (posterior) and trailing (anterior) part of a tooth. f) Light-microscope image of a semi-thin longitudinal section of a part of the radula of *P. caerulea* with the radular sac intact. The attachment of the tooth cusp to the radula by the tooth base can be clearly seen. g) Schematic representation demonstrating the self-sharpening arising from a gradient in hardness from the leading to the trailing side. The direction of tooth movement against the substrate is indicated by the blue arrow. Images a)–c) reproduced from, Ref. [116] d)–f) from Ref. [105] and g) from Ref. [101] with permission.

responsible for the superior mechanical properties of radular teeth. What is also common to both chitons and limpets is the terminology pertaining to the anatomy of the teeth, which is best described by observing a tooth 'in action' (Figure 4). The "front" tooth side used for scraping is called the leading part (alternatively also the posterior part), while the 'back' side which is not directly exposed to scraping is termed the trailing part (alternatively also the anterior part)[101,109] (Figure 4e). The part of the tooth which anchors to the radula is called the tooth base and the part used for scraping is commonly termed the cusp (Figure 4f).[101,109]

4.2. Structure and Function of Chiton Radular Teeth

Studies on numerous species have revealed that magnetite is found in the cusps of all chitons, whereas its distribution, as well as the presence of other iron and non-iron minerals is genus specific (Figure 5 and Refs. [4,109,110]). In maturing teeth there are various iron oxide phases deposited onto the preformed matrix, first in the junctional zone and on the outer margins and afterwards throughout most of the leading part, undergoing several phase transformations during maturation (see Figure 6).[101a,103,110d,111,112] In immature teeth, at the onset of mineralization, ferrihydrite (FH) is located in the junctional zone and later also on the outer margins of the tooth cusp[101a,103,110d,111] and persists in the leading part up to the very mature teeth.[103,112a,b] There, ferrihydrite is replaced by various iron oxide and iron oxyhydroxide mineral species,[4,103] generically magnetite (Figures 5, 6e–g, and 7), but genus- or species-specific forms, such as goethite (α-FeOOH),[111b,112c] lepidocrocite (γ-FeOOH)[110,112a,b,d,e] and the undifferentiated hydrated iron oxides under the name limonite[113] were observed as well, though in smaller fractions. The location inside the tooth (Figure 5), that is, at the contact of various phases, suggests that these "special" forms do not form 'by design', but most likely simply crystallize under altered conditions or in contact with locally specific interfaces.

In chiton *A. hirtosa*, Kim et al. found that ferrihydrite formed in immature teeth is replaced by a combination of

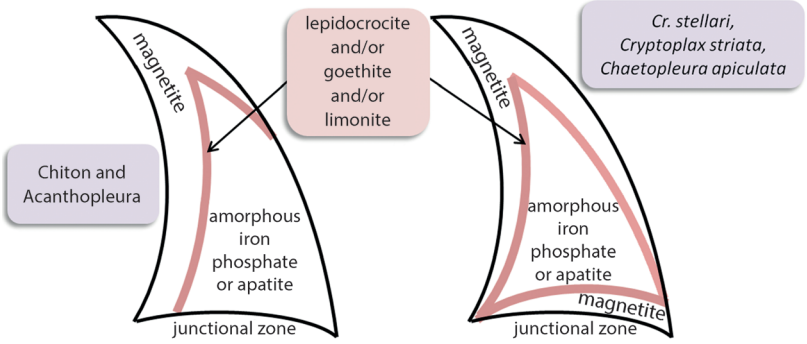

Figure 5. Schematic representation depicting the two main types of structure of chiton radular teeth with respect to the location of the magnetite veneer along with the genus or species where the type was observed.[4,109,110]

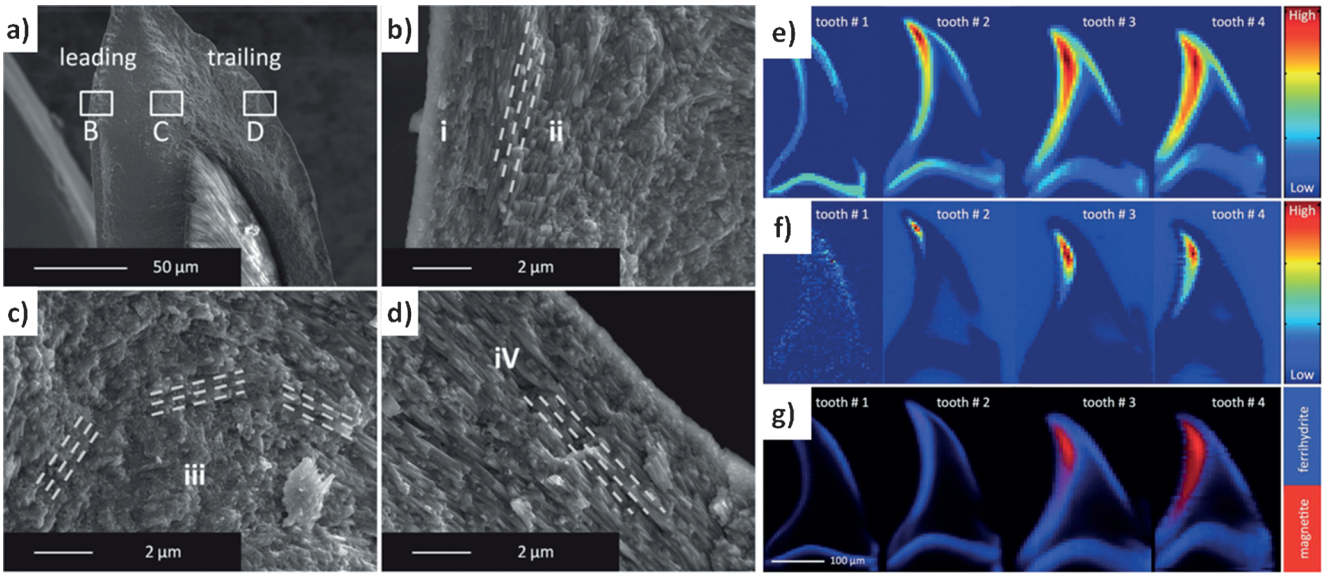

Figure 6. SEM image of a longitudinal fracture surface of a mature radular tooth of chiton *C. stellari* showing the iron phosphate core (lighter) and the magnetite shell regio (darker).The marked rectangles B,C, and D in (a) are magnified in (b), (c), and (d), respectively. The local structural heterogeneity includes (i) the granular magnetite veneer, the magnetite rods oriented parallel to the (ii) leading and (iv) trailing tooth edges and (iii) a gradual bending at transitional zone between them. The dashed lines illustrate the dominant local orientation of the rods in regions (ii), (iii), and (iv), e)–f) Micro X-ray fluorescence (µXRF) scans of longitudinal thin sections of radular teeth form *C. stellari*. The intensity of e) total iron and f) ferrous iron increase across the leading edge during tooth maturation. g) Micro X-ray absorption near-edge structure (µXANES) analysis shows an increasing abundance of magnetite across the shell region along the leading edge of radular teeth. Images reproduced from Ref. [116] with permission.

magnetite, lepidocrocite, and goethite in mature teeth.[111b] Moreover, the magnetite crystals in the leading part were found to be randomly oriented. Meanwhile, Evans et al. found that in the calcified tooth cores, the crystals either followed the orientation of organic matrix or formed interconnecting fibrous bridges.[108b] The tooth core is the region which is mineralized last, following a very complex pattern. Typically, it consists of either amorphous iron phosphate[114] or apatite,[4,112c,115] but more complex, Fe- and/or Mg-containing phases were observed as well.[112b,e]

More conclusive insight into the ultrastructure of chiton teeth was presented only recently for the radula of chiton *C. Stellari* using a combination of crystallographic, microscopic, and advanced spectroscopic techniques.[116] The mature teeth exhibited a locally segregated iron phosphate/magnetite core–shell structure. The outer shell region consisted either of magnetite particles or rods, where the rod axes were oriented along the contour of the tooth surface (see Figure 6a–d). Four morphological transitions were identified in the magnetite phase when going from the leading to the trailing edge of a tooth (Figure 6a–d): i) a thin layer of condensed magnetite nanoparticles surrounding the entire periphery of each tooth, which is thickened in the outermost part of the leading edge, ii) bundles of magnetite rods lying

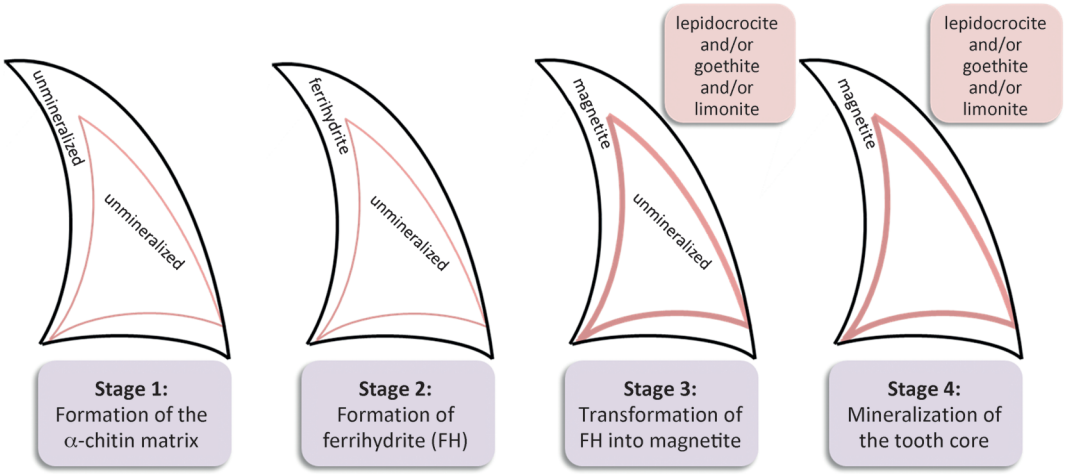

Figure 7. The four stages of tooth mineralization in the Chitonida according to Lowenstam and Weiner.[4]

beneath this layer, which were oriented parallel to the leading edge surface, iii) the local direction of the rods' orientation was gradually bent around the iron phosphate core up to the trailing edge, where iv) the orientation of the rods became parallel again to the trailing surface. The thickness of the rods gradually increased from the leading to the trailing edge, which was correlated with a significant decrease in hardness and modulus.[101a]

In a more recent study, reproducing and extending these previous results, Grunenfelder and co-workers have shown that smaller fibers are better suited for tensile loading because they have fewer flaws, and are therefore less brittle.[117] Conversely, they perform worse during compression, where thicker fibers are preferred. The observations led to the conclusion that the larger diameter rods observed on the trailing edge of the tooth are optimized to withstand the compressive loading concentrated in this region, whereas the thinner ones are optimized for tensile loading in the leading edge. The difference in moduli of the hard magnetite shell and the soft phosphate core was found to be large enough to enable crack-deflection at the core–shell interface, an effect also known from other (biological) composites.[118] Additionally, the presence of the organics surrounding each mineralized rod as well as the organic template within magnetite crystals (as a remnant of a templated nucleation) reduce the modulus and assure a higher hardness/modulus ratio, which facilitates an improved abrasion resistance when loading under blunt contact.[117]

At the nanoscale, surface asperities and mineral bridges were found as additional toughening mechanisms.[117] These structural features provide a detailed microscopic structural explanation for the supreme mechanical properties and the well-defined asymmetric wear patterns of the teeth enabling a self-sharpening condition[101a,102,117] (Figure 4 g). In addition, it had already been demonstrated that in contrast to the original ideas of Lowenstam and Weiner, who suggested that various mineral phases coexist in separate compartments,[4] different mineral phases instead interpenetrate with each other, thus blurring any sharp transitions between them.[112c,119] Combined, these findings hint at an even higher level of precision of spatio-temporal control over nucleation and growth of various coexisting mineral phases.

4.3. Mechanistic Aspects of Magnetite Biomineralization in Chiton Radular Teeth

The mineralization process of chiton teeth follows a complex pattern involving several morphological and phase transformations. In their work, Lowenstam and Weiner[4] described four generic stages of tooth mineralization in the chitonida (Figure 7): i) formation and organization of the organic matrix, ii) formation of a transient iron mineral iii) conversion of the transient iron mineral into other minerals. In the last stage, iv) mineralization occurs also in the tooth core. The four stages, as well as the (predominant) transformation of ferrihydrite to magnetite (Figure 7) are, in principle, common to all chitons. Beyond these commonalities, genus- or species-specific features have been observed, ranging from the mineral content and localization (Figure 5) to the proteins potentially involved in the mineralization process. Owing to the different methods used in various studies it is not clear whether any of the findings is generic for all chitons. We therefore specifically describe what we feel are the most important findings.

On extending the traditional mineralogical approaches to include biochemical analyses, it was shown that in chiton *A. hirtosa*, the preformed organic matrix undergoes phenolic hardening (also known as phenolic tanning and denotes the oxidation of phenolic compounds to quinones, which in turn react and cross-link proteins. The process increases the hardness of the tissue and produces a dark coloration) even prior to the onset of mineralization.[120] The same study revealed that around 10 % of the organic component is in fact proteins rich in acidic residues (aspartic and glutamic acid), which are suggested to be closely associated to the chitin fibers. The iron-mineral-containing outer regions of the tooth cusp were found to contain much less proteins than the calcified tooth core. In addition, chitin fibers in the iron-mineral-containing regions were found to be sparse and only purely ordered, while the calcified region contained densely packed and highly ordered rope-like fibers.[108b] Based on these results and along with the finding about the crystal orientations in the iron-containing and calcified regions,[108b] it was suggested that the mineralization in the calcified regions exhibits a much larger degree of control by the organic matrix than in the iron-containing region.[120]

The advance of characterization methods and an increasingly interdisciplinary approach enabled deeper insight and also demonstrated that the original models of mineralization of radula needed to be revised. Saunders et al. have shown that different mineral-containing regions are not separated by sharp, well-defined borders but instead interpenetrate each other.[112c] Moreover, even within regions containing the same minerals there are distinct inhomogeneities which ultimately give rise to self-sharpening properties.[101a] In the case of *C. stellari* the following series of structural transformations has been observed:[116] i) templated synthesis of ferrihydrite crystal aggregates along the preformed chitinous matrix followed by ii) an aggregation of crystal aggregates eventually undergoing a solid-state phase transformation from ferrihydrite to magnetite (see Figure 6 e–g), and iii) magnetite growth to form parallel rods in mature teeth.

In *A. hirtosa*, ferrihydrite was suggested to form by a redox mechanism from Fe^{II}.[111b] On the other hand, in *C. stellari* this redox mechanism was dismissed based on micro X-ray fluorescence (μXRF) data, because Fe^{II} was also present after deposition of ferrihydrite.[116] Instead, a mechanism was suggested involving hydrolysis of ferric iron to form positively charged ferric iron hydroxides, which should spontaneously precipitate in the form of ferrihydrite. This proposal is supported by the fact that the surface energy (and thus the barrier for nucleation) for hydrous phases is lower than for anhydrous phases, such as goethite, lepidocrocite, or akaganeite. The resulting metastable nanocrystalline ferrihydrite was in turn suggested to transform to magnetite by absorption of Fe^{II}.[121] Moreover, magnetite crystal aggregates were found to grow in a strikingly asymmetric manner, with

the grains on the perimeter of the aggregates growing more extensively than those in the cores.[116] Earlier proteomic analysis of the teeth had revealed several proteins specific for mineralized zones, one of them exhibiting homology with the C-terminal domain of a peroxiredoxin-6-like protein,[121b] which is known to be a reducing agent.[122,32] Based on these observations it was suggested that the proteins found in fully mineralized teeth could control the reduction of iron species and thereby control the initial phase transformation from ferrihydrite to magnetite by absorption of Fe^{II} and a subsequent solid-state transformation.[116] Moreover, the chitin matrix was suggested to influence the density of the magnetite crystal aggregate as well as the diameter and curvature of resulting rods. In addition, all the crystal aggregates were found to be in contact with chitin fibers, suggesting heterogeneous nucleation of initial ferrihydrite on the fibers.[116] Evidence for this idea has been collected in the case of *A. hirtosa*, where a peptide similar to the iron-binding protein Mms6 was extracted from mineralized teeth,[60,61,123] and was believed to be distributed on the chitin matrix where it may enhance ferrihydrite nucleation.[120] It thus appears very likely that protein-coated chitin fibers act as nucleating agents for heterogeneous nucleation of ferrihydrite. This idea was in turn supported by the observation that the crystal aggregates are smaller and the density is larger in the leading edge than in the trailing edge of mature teeth of *C. stellari*.[116] At the same time, the organic fibers are also more densely packed in the leading edge, which according to the above view, corresponds to a higher density of nucleation sites.[116] This situation indicates a very high degree of control over mineralization.

Strikingly, state-of-the-art atom-probe tomography analysis of radular teeth of *C. apiculata* revealed distinct local heterogeneities on the molecular scale.[124] Around the semi-crystalline α-chitin fibers, small domains were found in which cations (Na^+, Mg^{2+}, or both) cluster. These domains occur because the local amorphous chitinous domains exclude acidic proteins and thus also the cations.[124] Moreover, proximity histograms showed that the iron-mineral/organic fiber interfaces were not sharp but graded, such that on a length scale of 2–4 nm both phases coexisted, interpenetrating each other. The only cations co-localized with the fibers were either Na^+, Mg^{2+}, or both, suggesting the chitin-associated acidic proteins selectively attract the cations. It was further speculated that these localized specific ion affinities could regulate surface charges and that the local charge distributions govern the inter-fiber interactions and potentially also the onset of mineral nucleation by charge condensation. While there is no direct evidence for such mechanisms, the picture nevertheless points at an even more delicate level of control over nucleation and growth of iron oxide biominerals than originally thought.

4.4. Structure and Function of Limpet Radular Teeth

The mineralization of limpet radular teeth has been the subject of studies on various species, among them *Patella vulgata*,[101b,104,108a,125] *athletica*,[125a] *peronii*,[126] and *caerulea*,[105,127] as well as *Patelloida alticostata*[126] and *Cellana toreuma*.[128] While possibly displaying variation in the shapes and sizes of teeth, the studies revealed that the cusps are made of a preformed α-chitin matrix filled by goethite (α-FeOOH) and amorphous hydrated silica ($SiO_2{\cdot}nH_2O$), indicating a highly universal tooth cusp composition. In a broader context the formation of composite biomineralized materials is also referred to as "multiphase biomineralization"[5f] and is also known in other marine invertebrates, such as sponges[5f,129a] (chitin, silica and aragonite), brachiopods[5f,129b–c] (chitin, silica and apatite) and crustaceans[5f,129d] (chitin and silica).

In the limpet species *Patella vulgata*, *athletica*, and *caerulae*, the α-chitin matrix was found to consist of relatively well ordered, densely packed arrays of chitin fibers with only a few nanometers between adjacent fibers.[105] Results of histochemical studies revealed proteins alongside chitin and also suggested that, in these species as well, phenolic hardening occurs immediately prior to deposition of minerals.[108a] In the leading part, the α-chitin matrix fibers were found to be organized in two types of layers with a thickness ranging between 300 and 900 nm.[101b] Within these layers, which were positioned transverse to the leading surface, the fibers were oriented either parallel or perpendicular to the surface, arranged in an alternating fashion. In the trailing part, the fibers were found to be oriented perpendicular to the leading edge. At the border between the leading and trailing parts the fibers were shown to form a cross-shaped pattern (Figure 8a).

The first mineral products were observed on the base[105,125b,130] and correspond to poorly ordered mineral deposits of variable composition and size containing Fe, Si, P, and Ca.[125b,130] In the cusp the levels of P and Ca were very low compared to Fe and Si.[130b] In *Patella vulgata*, the first minerals deposits appeared in row 13[104] and in the case of *Patella caerulea* in row 19.[105] The first ordered mineral phase (goethite)[110a] appeared on the tooth base or at the junction of the tooth base and the tooth cusp.[104,108c,125b,131] The first minerals on the tooth cusp were found in the form of linear aggregates in contact with chitin fibers, which suggests that the fibers control crystal orientation.[105] Goethite forms as acicular crystals with the longer axis parallel to the fibers.[125b] On the basis of a highly heterogeneous crystal morphology the growth of crystals was suggested to be largely unaffected by the matrix.[105,127] The fact that the inter-fiber spacing inside the fiber-layers was found to be comparable to the crystal thickness and the finding that the crystallographic *c*-axes of goethite are oriented along the fibers,[101b] suggest that the organic matrix plays a regulatory role in crystal growth. The space between the goethite crystals becomes subsequently filled by hydrated silica.[101b,132] The formed goethite crystals have been studied by microscopic and spectroscopic techniques.[101b,125b,127,133] The tooth base was found to contain microcrystalline (superparamagnetic) and poorly ordered goethite, whereas the cusp contains acicular goethite crystals.[133] These acicular crystals are oriented along the fibers and are smaller in the leading part and larger in the trailing part.[101b]

While knowledge about the spatial distribution of mineral phases inside limpet teeth remains elusive, some information concerning the spatially resolved elemental composition has

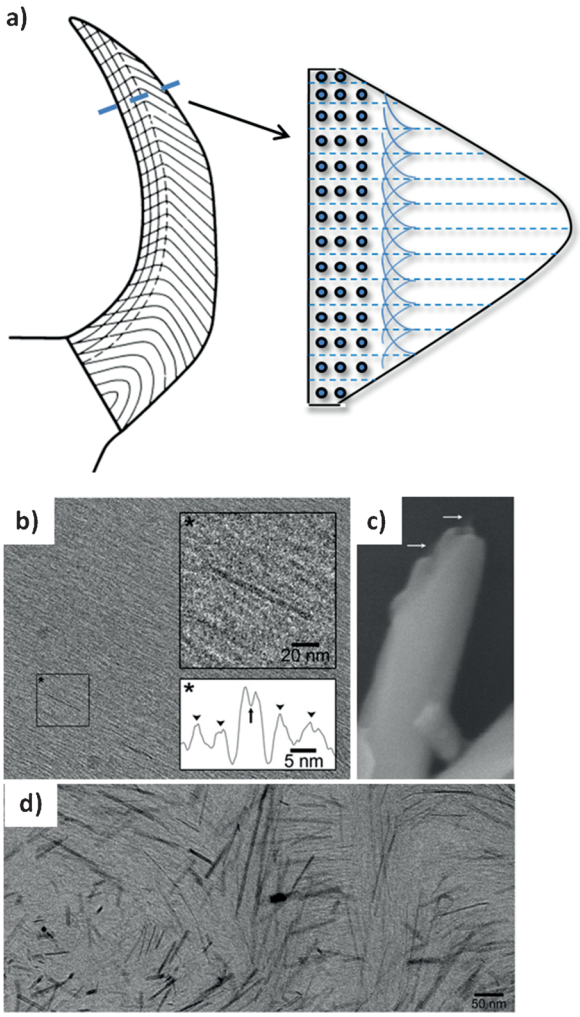

Figure 8. a) The orientation of the α-chitin fibers in a longitudinal (left) and transverse (right) cross-section of a radular tooth in limpet teeth. Left panel: lines denote the fibers; Right panel: Lines denote the fibers lying perpendicular to the leading edge and the dots depict those lying parallel to the edge. Near the trailing edge the fibers lie parallel to the edge while they form a cross pattern at the border between the leading and trailing edge. b)–d) TEM images of early mineral deposits in limpet *Patella caerulea*; some mineral deposits have an electron-lucent core. Inset of (b): A less under-focused TEM image, depicting fibers that are not as clear owing to the low contrast but with a better resolution. The intensity profile across such a particle reveals a dip in intensity in the middle of the particle (denoted by the arrow). The two arrowheads on each side of the arrow point to peaks arising from chitin fibers. c) A broken hollow crystal with a smaller structure emerging from the hole. It is not clear whether this structure is organic (arrows indicate an almost electron transparent and presumably organic material). d) TEM image showing mineral deposits lying parallel as well as perpendicular to the section. Electron-lucent particles are seen as well. b) and d) reproduced from Ref. [105] and c) from Ref. [127] with permission.

been obtained. It was shown that the leading part of the tooth contains more Fe than Si, while in the middle and lower trailing region of the cusp the percentage of Si is higher than Fe.[134] By measuring the hardness of samples obtained after selective removal of the organic and mineral phases, respectively, it was demonstrated that the organic matrix plays merely a subordinate role for the hardness of mature teeth.[101b] Silica, on the other hand, was shown to be vital for the hardness.[101b] It was suggested that silica acts as cement for goethite crystals which are in the form of loose grains.[101b] In addition, the teeth were shown to display a well-defined plane of wear parallel to the elongation of the trailing part of the tooth.[101b] The orientation of this plane remains constant and assures a self-sharpening of the tooth, analogous to observations in chiton radulae.[101b] The self-sharpening, as well as a high resistance against the propagation of cracks in the tooth is enabled by the hierarchical ultrastructural organization.[101b] The spatial resolution of phases aside, all results have shown that goethite is the only iron mineral observed, that is, it does not appear to form an amorphous precursor.

The organizational and compositional differences with respect to chiton teeth result in a lower hardness of mature teeth (an average Vickers hardness of 676 $kg\,m^{-1}\,m^{-2}$ in chitons compared to 413 $kg\,m^{-1}\,m^{-2}$ in limpets).[102] The microscopic origin of this difference in hardness remains, however, elusive.

4.5. Mechanistic Aspects of Goethite Mineralization in Limpets

There are several important mechanistic questions that have received much attention in the past, but nevertheless still remain open. Compared to chitons, the biomineralization of limpet radula is not understood in such detail. The most striking questions are related to the formation pathway of goethite, in particular the absence of a transient amorphous precursor and the reaction itself.

In the teeth, no pre-formed compartments were observed which could possibly control crystal size and shape.[105] Instead, the crystals apparently push aside or engulf the fibers as they grow. It appears that the mineralization of the base is not under appreciable biological control. Conversely, the mineralization of the cusp appears to be under strict biological control. Some goethite crystals were found to be either hollow or to contain an organic core (Figure 8b–d), suggesting, at least in part, a heterogeneous crystal nucleation on the organic matrix.[101b,105,127] These crystals have a thickness comparable to a unit cell and still have well-recognizable crystal faces and display various crystal habits (Figure 8c,d).[105,127] It is suggested that interactions with organic fibers stabilize these structures long enough to make them experimentally observable during their growth.[127] Some crystals were found to display triangular morphology, which is possible only by breaking the symmetry of the *Pbnm* space group.[127] The symmetry breaking was attributed to nucleation of crystals on the fibers, which would prevent the growth of symmetry-related faces.[105,127] Similar morphological symmetry reduction was also observed in vitro, in crystallization studies in the presence of additives[135] and indicates a certain level of biological control over nucleation.[127]

Moreover, it is well established that goethite does not crystallize spontaneously from Fe^{III} in aqueous solutions, at neutral pH, and close to physiological conditions.[136] The only path to forming goethite crystals at ambient conditions is

through in situ oxidation of Fe^{II}.[136b,137] The crystals formed by such oxidative hydrolysis, however, generally do not have well-defined morphologies such as those found in limpet teeth. All synthetic routes to goethite crystallization involve extreme pH values, elevated temperature or both.[136] In these processes, a poorly crystalline ferrihydrite precursor phase is deposited first and long incubation times are required for its subsequent transformation into goethite. In the limpet teeth, no such ferrihydrite precursor phase has ever been detected.[101b,105,127] The limpet was thus suggested to either avoid the formation of metastable precursors entirely or to somehow shorten the time-window in which they are stable and observable.[105] All the studies to date (on various species) report an absence of an amorphous precursor of any kind.[101b,105,127] In any case, the direct deposition of goethite indicates a considerable biological control over goethite biomineralization in limpet teeth. Moreover, lepidocrocite (γ-FeOOH), while thermodynamically less stable, is often kinetically favored in precipitation reactions. Goethite formation is favored when the rate of oxidation of Fe^{II} is very slow, such as in presence of CO_2/HCO_3^-,[137a] Mn^{2+}[138] or Al^{3+}.[137a] It was thus speculated that the biomineralization mechanism in limpet teeth could involve slow oxidative hydrolysis favoring goethite over lepidocrocite formation for controlled nucleation governed by the organic matrix.[125b] In turn, the organic matrix framework is speculated to be coated by (acidic) proteins which would act as nucleating centers.[105] The speculations aside, in the case of limpets, the proteins (potentially) involved in biomineralization remain elusive and the protein control over goethite nucleation is still an unexplored territory.

The possibility of changes in fiber dimensions and/or inter-fiber spacing triggering and controlling goethite nucleation has also not yet been ruled out.[105] In addition, it was shown that soluble Si has an inhibitory effect on goethite mineralization,[139] yet in all stages of goethite mineralization in the radular teeth of *Patella vulgata* significant amounts of Si have been detected.[125b,130a,133] It appears that only in mature and fully mineralized teeth is Si incorporated in an inert silica phase and that during the mineralizing stages Si exists in a soluble form, which was suggested to exert some regulatory function in connection with the chitin matrix.[101b]

The second intriguing question concerns iron transport into and inside the tooth. Several studies have not revealed any presence of ferritin cores within limpet teeth.[105,128,133] Occasionally ferritin cores were observed adjacent to the tooth, but never inside.[105] Similar observations were made in chitons, where it was suggested that ferritin cores must be dissolved prior to transportation across the cell membrane into the tooth.[2] Supporting this idea is the finding that in chiton teeth, the degree of crystallinity of the initial ferrihydrite deposits is greater than the that of the ferritin cores in the teeth-adjacent cells.[111b] The current opinion therefore remains that in limpets as well, iron enters the tooth in a soluble form.[105] In addition, the finding that in the early stages of mineralization the parts that are more distant from the leading edge are more intensively mineralized than the ones near the edge[105,108c] triggered speculations that the early mineral deposits at the junction between the base and the cusp could serve as a reservoir for the mineralization of the cusp.[105] Moreover, since free iron in the cytosol is toxic (i.e., it can catalyze the formation of hydroxyl radicals), it was suggested that it could be located in a vacuole undergoing exocytosis just like the free iron in the vacuole of the transferrin endosome.[140] Results of immunolabeling studies of radulae of *Cellana toreuma* revealed that a 26 kDa ferritin subunit is in fact translocated across the cell membrane into the teeth.[128] It was speculated that the detected disassembled ferritin subunit released free iron and/or partially degraded ferritin into the tooth after fusion of a lysosome-like vacuole with the cell membrane.[128] The mechanism of how iron is protected and transported across the tooth remains unclear.

4.6. Open Questions

While great activity in the research field shed light on several aspects of biomineralization of both chiton and limpet radula, several mechanistic questions remain open and still need to be addressed in more detail. From a fundamental point of view, the most crucial one in the case of chitons is certainly related to the molecular picture of templating mechanisms, suggested to be mediated by, presumably acidic, proteins. In vitro experiments indeed suggest an important role of acidic ligands in the formation of ferrihydrite[141] and suppression of lepidocrocite formation.[142] In addition, poly(aspartic acid) was found to have a multi-modal effect on ferrihydrite formation.[143] Several protein species were identified, which are homologous with known proteins with, for example, enzymatic activity.[60,61,116,123] In addition, no direct evidence has been given about whether and how these proteins actually affect the nucleation and growth stages. Thus, these findings remain circumstantial and the spatio-temporally resolved identity of the nucleation-controlling proteins, along with the actual molecular mechanism of their action, remains unknown and thus a matter of speculation. To eventually be exploited for strategies towards preparing modern multifunctional synthetic materials, ideas such as molecular control over crystallization with exceedingly small concentrations of 'additives', demand further mechanistic insight.

Compared to chitons, much less mechanistic insight is at hand for limpets. Typical of the problems perplexing researchers in the field is the elusive reaction pathway for the formation of goethite crystals under physiological conditions from Fe^{II}, this question in turn is entangled with the issue of the protection and transport of free iron into and across the tooth. As in chitons, extensive speculations were made about chitin-associated proteins controlling nucleation and growth of goethite crystals. Yet, such proteins in limpets have not been identified and their mode of action remains unknown. Similar holds true for the events triggering goethite precipitation, be it changes in chitin inter-fiber spacing, sudden changes in iron delivery, or something entirely different. In addition, the speculation about the absence of control over the growth of goethite crystals (displaying very heterogeneous morphology) is contradicted by their clear preferential orientation. Namely, it is known from studies of

crystallization in porous materials that in absence of considerable heterogeneous nucleation and growth on pore walls, the growing particles exert large local stresses on pore walls.[144] Applying these ideas to uncontrolled crystal growth in the presence of chitin fiber bundles local deformations in fiber structure and alignment are expected to be observed, but these have apparently not been observed. Thus, growth might be controlled as well, either directly by interaction with fibers or perhaps by control of local iron delivery. More intensive interdisciplinary studies are thus called for to give a more complete picture about goethite biomineralization in limpet radular teeth.

5. Summary and Outlook

New information is obtained on a daily basis with respect to biological macromolecules involved in biomineralization, thanks to the advance of new analytical techniques, and specifically, new sequencing techniques. However, there is still a long way to go towards a complete understanding of biomineralization pathways and being able to profit from them in terms of biomimetics for the formation of functional and self-repairing materials. In particular, the field needs even greater interaction between scientists from diverse fields to jointly tackle challenging problems that cannot be solved solely from one perspective.

In the specific 'world' of iron oxide biomineralization, the genes and proteins involved in magnetite formation in magnetotactic bacteria are mostly known, but efforts are needed to understand their dedicated mechanistic role. Such information is completely absent in the case of the mollusks, but with the development of sequencing techniques, genetic information will hopefully become accessible in the near future to complement the elaborate physico-chemical work done to date. In particular, the much larger scales and quantities of iron minerals involved in these higher organisms evidently require a more complex, multi-level control over mineralization. At the same time, larger or even bulk quantities are also required for efficient biomimetic materials production. Compared to the intensively studied calcium minerals,[9d] the biomimetic approaches of depositing iron oxide biominerals[9e–h,85] are still underdeveloped. These in situ studies would offer a deeper mechanistic insight into iron oxide mineralization. Beyond their conceptual value the in situ studies have already proven extremely successful in the field of biomimetic and bioinspired optical materials,[145] which should inspire more biomimetic studies on iron oxide mineralization, both fundamental as well as practically oriented. Therefore, the more detailed, molecular-scale knowledge obtained from magnetotactic bacteria should inspire and promote equivalent efforts in higher organisms such as limpets and chitons. A detailed understanding of the hierarchical multi-level control over iron oxide mineral deposition on a molecular level in these higher organisms would pave the way towards a programmable, molecularly controlled, smart, biomimetic materials design.

We thank Arash Komeili and Dirk Schüler for their introduction to the world of biomineralization in general and magnetotactic bacteria in particular. We thank Peter Fratzl for helping in the establishment of a research group at the MPI of Colloids and Interfaces. We thank our colleagues from the group for their daily help and in particular Matthew Hood for the "native speaker improvement of our text". Financial support to D.F. from the Deutsche ForschungsGemeinschaft (SPP 1420 (FA 835/2), SPP 1569 (FA 835/5), SPP 1726 (FA 835/7), and projects "Ein biokombinatorischer Ansatz zu enzymatisch aktivierbaren Klebstoffen"(BO 1762/5) and "Untersuchung des Ablaufes der Kalzitbiomineralisation in Coccolithophoren" (FA 835/9)), from the European Union (Project Bio2-MaN4MRI no. 245542 and Nanoathero no. 305312), from COST (no. 0902) and the European Research Council (Starting Grant MB2 no. 256915) is acknowledged. Experimental support was offered by the Collaborative Optical Spectroscopy, Micromanipulation and Imaging Centre within the framework of the European Soft Matter Infrastructure (Edinburgh, UK), and by diverse beamlines at the European Synchrotron Radiation Facility (Grenoble, France), SOLEIL (Scientific Pole of Saclay, France) and at the BESSY II Synchrotron (Berlin, Germany).

How to cite: *Angew. Chem. Int. Ed.* **2015**, *54*, 4728–4747
Angew. Chem. **2015**, *127*, 4810–4829

[1] E. Haeckel, *Kunstformen der Natur*, **1899**.
[2] H. A. Lowenstam, *Science* **1981**, *211*, 1126–1131.
[3] H. C. W. Skinner, *Mineral. Mag.* **2005**, *69*, 621–641.
[4] H. A. Lowenstam, S. Weiner, *On Biomineralization*, **1989**.
[5] a) P. Fratzl, J. W. C. Dunlop, R. Weinkamer, *Materials Design Inspired by Nature*: *Function Through Inner Architecture*, Vol. 1, The Royal Society of Chemistry, Cambridge, **2013**; b) P. Fratzl, *J. R. Soc. Interface* **2007**, *4*, 1–6; c) J. Aizenberg, J. C. Weaver, M. S. Thanawala, V. C. Sundar, D. E. Morse, P. Fratzl, *Science* **2005**, *309*, 275–278; d) A. Fischer, M. Schmitz, B. Aichmayer, P. Fratzl, D. Faivre, *J. R. Soc. Interface* **2011**, *8*, 1011–1018; e) P. Fratzl, R. Weinkamer, *Prog. Mater. Sci.* **2007**, *52*, 1263–1334; f) H. Ehrlich, *Biological Materials of Marine Origin: Invertebrates (Biologically-Inspired Systems)*, Springer, Heidelberg, **2010**.
[6] A. M. Belcher, X. H. Wu, R. J. Christensen, P. K. Hansma, G. D. Stucky, D. E. Morse, *Nature* **1996**, *381*, 56–58.
[7] B. Devouard, M. Pósfai, X. Hua, D. A. Bazylinski, R. B. Frankel, P. R. Buseck, *Am. Mineral.* **1998**, *83*, 1387–1398.
[8] a) E. Baeuerlein, *The Biology of Biominerals Structure Formation*, Vol. 1, Wiley-VCH, Weinheim, **2007**; b) E. Baeuerlein, P. Behrens, *Biomimetic and Bio-Inspired Materials Chemistry*, Vol. 2, Wiley-VCH, Weinheim, **2007**; c) E. Baeuerlein, M. Epple, *Biomineralization in Medicine*, Vol. 3, Wiley-VCH, Weinheim, **2007**; d) J. W. C. Dunlop, P. Fratzl, *Annu. Rev. Mater. Res.* **2010**, *40*, 1–24; e) S. Weiner, P. M. Dove, *Rev. Mineral. Geochem.* **2003**, *54*, 1–29.
[9] a) F. Nudelman, N. A. J. M. Sommerdijk, *Angew. Chem. Int. Ed.* **2012**, *51*, 6582–6596; *Angew. Chem.* **2012**, *124*, 6686–6700; b) S. Mann, *Biomineralization*: *Principles and Concepts in Bioinorganic Materials Chemistry*, Vol. 5, Oxford University Press, Oxford, **2001**; c) T. Klaus-Joerger, R. Joerger, E. Olsson, C.-G. Granqvist, *Trends Biotechnol.* **2001**, *19*, 15–20; d) E. Djuradin, S. Mann, *Adv. Funct. Mater.* **2002**, *14*, 1–14; e) T. Pozorov et al., *Adv. Funct. Mater.* **2007**, *17*, 951–957; f) E. D. Sone, S. I. Stupp, *Chem. Mater.* **2011**, *23*, 2005–2007; g) M. Nesterova, J. Moreau, J. F. Banfield, *Geochim. Geophys. Acta*

2003, *67*, 1185 – 1195; h) C. S. Chan et al., *Geochimica et Cosmochimica Acta* **2009**, *73*, 3807 – 3818.
[10] T. Prozorov, D. A. Bazylinski, S. K. Mallapragada, R. Prozorov, *Mater. Sci. Eng. R* **2013**, *74*, 133 – 172.
[11] R. B. Frankel, D. A. Bazylinski, *Rev. Mineral. Geochem.* **2003**, *54*, 95 – 114.
[12] a) A. C. Lasaga, *Kinetic theory in the earth sciences*, Princeton University Press, Princeton, **1998**; b) A. C. Lasaga, A. Lüttge, *Am. Mineral.* **2004**, *89*, 527 – 540; c) H. H. Teng, *Elements* **2013**, *9*, 189 – 194.
[13] a) J. Seto, Y. Ma, S. A. Davis, F. Meldrum, A. Gourrier, Y.-Y. Kim, U. Schilde, M. Sztucki, M. Burghammer, S. Maltsev, C. Jäger, H. Cölfen, *Proc. Natl. Acad. Sci. USA* **2012**, *109*, 3699 – 3704; b) Y. Politi, T. Arad, E. Klein, S. Weiner, L. Addadi, *Science* **2004**, *306*, 1161 – 1164; c) H. Cölfen, M. Antonietti, *Mesocrystals and Nonclassical Crystallization*, Wiley, Chichester, **2008**; d) J. Baumgartner, G. Morin, N. Menguy, T. P. Gonzalez, M. Widdrat, J. Cosmidis, D. Faivre, *Proc. Natl. Acad. Sci. USA* **2013**, *110*, 14883 – 14888.
[14] A. Navrotsky, *Proc. Natl. Acad. Sci. USA* **2004**, *101*, 12096 – 12101.
[15] P. Arosio, R. Ingrassia, P. Cavadini, *Biochim. Biophys. Acta Gen. Subj.* **2009**, *1790*, 589 – 599.
[16] a) S. Bellini, *Chin. J. Oceanol. Limnol.* **2009**, *27*, 3 – 5; b) S. Bellini, *Chin. J. Oceanol. Limnol.* **2009**, *27*, 6 – 12.
[17] R. P. Blakemore, *Science* **1975**, *190*, 377 – 379.
[18] a) D. S. McKay, E. K. Gibson, Jr., K. L. Thomas-Keprta, H. Vali, C. S. Romanek, S. J. Clemett, X. D. F. Chilier, C. R. Maechling, R. N. Zare, *Science* **1996**, *273*, 924 – 930; b) R. Massart, *IEEE Trans. Magn.* **1981**, *17*, 1247 – 1248.
[19] a) D. Murat, A. Quinlan, H. Vali, A. Komeili, *Proc. Natl. Acad. Sci. USA* **2010**, *107*, 5593 – 5598; b) K. Grünberg, C. Wawer, B. M. Tebo, D. Schüler, *Appl. Environ. Microbiol.* **2001**, *67*, 4573 – 4582; c) A. Scheffel, A. Gärdes, K. Grünberg, G. Wanner, D. Schüler, *J. Bacteriol.* **2008**, *190*, 377 – 386; d) D. Schüler, E. Baeuerlein, *Arch. Microbiol.* **1996**, *166*, 301 – 307.
[20] a) C. Lang, D. Schüler, D. Faivre, *Macromol. Biosci.* **2007**, *7*, 144 – 151; b) T. Matsunaga, T. Suzuki, M. Tanaka, A. Arakaki, *Trends Biotechnol.* **2007**, *25*, 182 – 188.
[21] C. T. Lefèvre, D. A. Bazylinski, *Microbiol. Mol. Biol. Rev.* **2013**, *77*, 497 – 526.
[22] Y. A. Gorby, T. J. Beveridge, R. Blakemore, *J. Bacteriol.* **1988**, *170*, 834 – 841.
[23] a) B. Devouard, M. Pósfai, X. Hua, D. A. Bazylinski, R. B. Frankel, P. B. Buseck, *Am. Mineral.* **1998**, *83*, 1387 – 1398; b) B. Arató, Z. Szanyi, C. B. Flies, D. Schüler, R. B. Frankel, P. R. Buseck, M. Pósfai, *Am. Mineral.* **2005**, *90*, 1233 – 1241.
[24] K. L. Thomas-Keprta, D. A. Bazlinski, J. L. Kirschvink, S. J. Clemett, D. S. McKay, S. J. Wentworth, H. Vali, E. K. Gibson, Jr., C. S. Romanek, *Geochim. Cosmochim. Acta* **2000**, *64*, 4049 – 4081.
[25] a) A. R. Muxworthy, W. Williams, *J. Geophys. Res.* **2006**, *111*, B12S12; b) A. R. Muxworthy, W. Williams, *J. R. Soc. Interface* **2009**, *6*, 1207 – 1212.
[26] A. Körnig, M. Winklhofer, J. Baumgartner, T. P. Gonzalez, P. Fratzl, D. Faivre, *Adv. Funct. Mater.* **2014**, *24*, 3926 – 3932.
[27] a) M. Bennet, A. McCarthy, D. Fix, M. R. Edwards, F. Repp, P. Vach, J. W. C. Dunlop, M. Sitti, G. S. Buller, S. Klumpp, D. Faivre, *PLoS One* **2014**, *9*, e101150; b) C. T. Lefèvre, M. Bennet, L. Landau, P. Vach, D. Pignol, D. A. Bazylinski, R. B. Frankel, S. Klumpp, D. Faivre, *Biophys. J.* **2014**, *107*, 527 – 538; c) R. B. Frankel, D. A. Bazylinski, M. S. Johnson, B. L. Taylor, *Biophys. J.* **1997**, *73*, 994 – 1000.
[28] R. B. Frankel, T. J. Williams, D. A. Bazylinski in *Magnetoreception and magnetosomes in bacteria*, Vol. 3 (Ed.: D. Schüler), Springer, Heidelberg, **2007**, pp. 1 – 24.
[29] R. B. Frankel, R. Blakemore, R. S. Wolfe, *Science* **1979**, *203*, 1355 – 1356.
[30] a) S. Mann, N. H. C. Sparks, R. B. Frankel, D. A. Bazlinski, H. W. Jannasch, *Nature* **1990**, *343*, 258 – 261; b) M. Farina, D. M. S. Esquivel, H. L. de Barros, *Nature* **1990**, *343*, 256 – 258.
[31] a) D. A. Bazylinski, B. R. Heywood, S. Mann, R. B. Frankel, *Nature* **1993**, *366*, 218; b) C. T. Lefèvre, N. Menguy, F. Abreu, U. Lins, M. Pósfai, T. Prozorov, D. Pignol, R. B. Frankel, D. A. Bazylinski, *Science* **2011**, *334*, 1720 – 1723.
[32] a) M. Pósfai, P. R. Buseck, D. A. Bazylinski, R. B. Frankel, *Science* **1998**, *280*, 880 – 883; b) M. Pósfai, P. R. Buseck, D. A. Bazylinski, R. B. Frankel, *Am. Mineral.* **1998**, *83*, 1469 – 1481.
[33] K. W. Mandernack, D. A. Bazylinski, W. C. Shanks, T. D. Bullen, *Science* **1999**, *285*, 1892 – 1896.
[34] D. Faivre, L. H. Böttger, B. F. Matzanke, D. Schüler, *Angew. Chem. Int. Ed.* **2007**, *46*, 8495 – 8499; *Angew. Chem.* **2007**, *119*, 8647 – 8652.
[35] a) R. B. Frankel, G. C. Papaefthymiou, R. P. Blakemore, W. O'Brien, *Biochim. Biophys. Acta* **1983**, *763*, 147 – 159; b) S. Staniland, B. Ward, A. Harrison, G. van der Laan, N. Telling, *Proc. Natl. Acad. Sci. USA* **2007**, *104*, 19524 – 19528.
[36] M. L. Fdez-Gubieda, A. Muela, J. Alonso, A. García-Prieto, L. Olivi, R. Fernández-Pacheco, J. M. Barandiarán, *ACS Nano* **2013**, *7*, 3297 – 3305.
[37] a) C. Quintana, J. M. Cowley, C. Marhic, *J. Struct. Biol.* **2004**, *147*, 166 – 178; b) Y. H. Pan, K. Sader, J. J. Powell, A. Bleloch, M. Gass, J. Trinick, A. Warley, A. Li, R. Brydson, A. Brown, *J. Struct. Biol.* **2009**, *166*, 22 – 31.
[38] M. E. Byrne, D. A. Ball, J.-L. Guerquin-Kern, I. Rouiller, T.-D. Wu, K. H. Downing, H. Vali, A. Komeili, *Proc. Natl. Acad. Sci. USA* **2010**, *107*, 12263 – 12268.
[39] a) D. Faivre, A. Fischer, I. Garcia-Rubio, G. Mastrogiacomo, A. U. Gehring, *Biophys. J.* **2010**, *99*, 1268 – 1273; b) D. Faivre, N. Menguy, M. Pósfai, D. Schüler, *Am. Mineral.* **2008**, *93*, 463 – 469; c) C. Carvallo, S. Hickey, D. Faivre, N. Menguy, *Earth Planets Space* **2009**, *61*, 143 – 145.
[40] a) Y. Okuda, K. Denda, Y. Fukumori, *Gene* **1996**, *171*, 99 – 102; b) K. Grünberg, E. C. Müller, A. Otto, R. Reszka, D. Linder, M. Kube, R. Reinhardt, D. Schüler, *Appl. Environ. Microbiol.* **2004**, *70*, 1040 – 1050; c) M. Tanaka, Y. Okamura, A. Arakaki, T. Tanaka, H. Takeyama, T. Matsunaga, *Proteomics* **2006**, *6*, 5234 – 5247.
[41] a) A. Komeili, Z. Li, D. K. Newman, G. J. Jensen, *Science* **2006**, *311*, 242 – 245; b) E. Katzmann, F. D. Müller, C. Lang, M. Messerer, M. Winklhofer, J. M. Plitzko, D. Schüler, *Mol. Microbiol.* **2011**, *82*, 1316 – 1329.
[42] C. Jogler, D. Schüler, *Annu. Rev. Microbiol.* **2009**, *63*, 501 – 521.
[43] S. Schübbe, M. Kube, A. Scheffel, C. Wawer, U. Heyen, A. Meyerdierks, M. Madkour, F. Mayer, R. Reinhardt, D. Schüler, *J. Bacteriol.* **2003**, *185*, 5779 – 5790.
[44] S. Ullrich, M. Kube, S. Schübbe, R. Reinhardt, D. Schüler, *J. Bacteriol.* **2005**, *187*, 7176 – 7184.
[45] a) C. Jogler, W. Lin, A. Meyerdierks, M. Kube, E. Katzmann, C. Flies, Y. Pan, R. Amann, R. Reinhardt, D. Schuler, *Appl. Environ. Microbiol.* **2009**, *75*, 3972 – 3979; b) C. Jogler, G. Wanner, S. Kolinko, M. Niebler, R. Amann, N. Petersen, M. Kube, R. Reinhardt, D. Schüler, *Proc. Natl. Acad. Sci. USA* **2011**, *108*, 1134 – 1139.
[46] F. Abreu, M. E. Cantao, M. F. Nicolas, F. G. Barcellos, V. Morillo, L. G. P. Almeida, F. F. do Nascimento, C. T. Lefevre, D. A. Bazylinski, A. T. R. de Vasconcelos, U. Lins, *ISME J.* **2011**, *5*, 1634 – 1640.
[47] A. Lohße, S. Ullrich, E. Katzmann, S. Borg, G. Wanner, M. Richter, B. Voigt, T. Schweder, D. Schüler, *PLoS One* **2011**, *6*, e25561.

[48] D. Murat, V. Falahati, L. Bertinetti, R. Csencsits, A. Körnig, K. H. Downing, D. Faivre, A. Komeili, *Mol. Microbiol.* **2012**, *85*, 684 – 699.
[49] M. Richter, M. Kube, D. A. Bazylinski, T. Lombardot, F. O. Glockner, R. Reinhardt, D. Schüler, *J. Bacteriol.* **2007**, *189*, 4899 – 4910.
[50] A. Lohße, S. Borg, O. Raschdorf, I. Kolinko, E. Tompa, M. Pósfai, D. Faivre, J. Baumgartner, D. Schüler, *J. Bacteriol.* **2014**, *196*, 2658 – 2669.
[51] I. Kolinko, A. Lohsze, S. Borg, O. Raschdorf, C. Jogler, Q. Tu, M. Pósfai, E. Tompa, J. M. Plitzko, A. Brachmann, G. Wanner, R. Müller, Y. Zhang, D. Schüler, *Nat. Nanotechnol.* **2014**, *9*, 193 – 197.
[52] R. Uebe, K. Junge, V. Henn, G. Poxleitner, E. Katzmann, J. M. Plitzko, R. Zarivach, T. Kasama, G. Wanner, M. Pósfai, L. Böttger, B. F. Matzanke, D. Schüler, *Mol. Microbiol.* **2011**, *82*, 818 – 835.
[53] A. Komeili, *FEMS Microbiol. Rev.* **2012**, *36*, 232 – 255.
[54] S. C. Andrews, A. K. Robinson, F. Rodriguez-Quinones, *FEMS Microbiol. Rev.* **2003**, *27*, 215 – 237.
[55] a) R. J. Calugay, H. Miyashita, Y. Okamura, T. Matsunaga, *FEMS Microbiol. Lett.* **2003**, *218*, 371 – 375; b) R. J. Calugay, Y. Okamura, A. T. Wahyudi, H. Takeyama, T. Matsunaga, *Biochem. Biophys. Res. Commun.* **2004**, *323*, 852 – 857; c) R. J. Calugay, H. Takeyama, D. Mukoyama, Y. Fukuda, T. Suzuki, K. Kanoh, T. Matsunaga, *J. Biosci. Bioeng.* **2006**, *101*, 445 – 447.
[56] H. Yijun, Z. Weijia, J. Wei, R. Chengbo, L. Ying, *Biochemistry* **2007**, *72*, 1247 – 1253.
[57] a) R. Uebe, B. Voigt, T. Schweder, D. Albrecht, E. Katzmann, C. Lang, L. Bottger, B. F. Matzanke, D. Schüler, *J. Bacteriol.* **2010**, *192*, 4192 – 4204; b) L. Qi, J. Li, W. Zhang, J. Liu, C. Rong, Y. Li, L. Wu, *PLoS One* **2012**, *7*, e29572.
[58] M. I. Siponen, P. Legrand, M. Widdrat, S. R. Jones, W.-J. Zhang, M. C. Y. Chang, D. Faivre, P. Arnoux, D. Pignol, *Nature* **2013**, *502*, 681 – 684.
[59] a) O. Raschdorf, F. D. Müller, M. Pósfai, J. M. Plitzko, D. Schüler, *Mol. Microbiol.* **2013**, *89*, 872 – 886; b) J. Yang, S. Li, X. Huang, J. Li, L. Li, Y. Pan, Y. Li, *BMC Microbiol.* **2013**, *13*, 203.
[60] W. Yang, R. Li, T. Peng, Y. Zhang, W. Jiang, Y. Li, J. Li, *Res. Microbiol.* **2010**, *161*, 701 – 705.
[61] N. Zeytuni, E. Ozyamak, K. Ben-Harush, G. Davidov, M. Levin, Y. Gat, T. Moyal, A. Brik, A. Komeili, R. Zarivach, *Proc. Natl. Acad. Sci. USA* **2011**, *108*, E480 – E487.
[62] a) See Ref. [53]; b) H. Nakazawa, A. Arakaki, S. Narita-Yamada, I. Yashiro, K. Jinno, N. Aoki, A. Tsuruyama, Y. Okamura, S. Tanikawa, N. Fujita, H. Takeyama, T. Matsunaga, *Genome Res.* **2009**, *19*, 1801 – 1808.
[63] See Ref. [19c].
[64] A. Arakaki, J. Webb, T. Matsunaga, *J. Biol. Chem.* **2003**, *278*, 8745 – 8750.
[65] M. Tanaka, E. Mazuyama, A. Arakaki, T. Matsunaga, *J. Biol. Chem.* **2011**, *286*, 6386 – 6392.
[66] A. Lohße, S. Ullrich, E. Katzmann, S. Borg, G. Wanner, M. Richter, B. Voigt, T. Schweder, D. Schüler, *PLoS One* **2011**, *6*, e25561.
[67] J. Wang, Z. Peng, Y. Huang, Q. Chen, *J. Cryst. Growth* **2004**, *263*, 616 – 619.
[68] a) Y. Amemiya, A. Arakaki, S. S. Staniland, T. Tanaka, T. Matsunaga, *Biomaterials* **2007**, *28*, 5381 – 5389; b) A. Arakaki, F. Masuda, Y. Amemiya, T. Tanaka, T. Matsunaga, *J. Colloid Interface Sci.* **2010**, *343*, 65 – 70.
[69] D. Faivre, N. Menguy, F. Guyot, O. Lopez, P. Zuddas, *Am. Mineral.* **2005**, *90*, 1793 – 1800.
[70] R. Frankel, T. Williams, D. Bazylinski, *Magnetoreception and magnetosomes in bacteria*, Vol. 3 (Ed.: D. Schüler), Springer, Berlin/Heidelberg, **2007**, pp. 1 – 24.
[71] J. L. Kirschvink, *Earth Planetary Sci. Lett.* **1982**, *59*, 388 – 392.
[72] A. Körnig, J. Dong, M. Bennet, M. Widdrat, J. Andert, F. D. Müller, D. Schüler, S. Klumpp, D. Faivre, *Nano Lett.* **2014**, 4653 – 4659.
[73] a) A. Scheffel, M. Gruska, D. Faivre, A. Linaroudis, J. M. Plitzko, D. Schüler, *Nature* **2006**, *440*, 110 – 115; b) See Ref. [41a].
[74] R. B. Frankel, D. A. Bazylinski, *Trends Microbiol.* **2006**, *14*, 329 – 331.
[75] S. Schübbe, C. Würdemann, J. Peplies, U. Heyen, C. Wawer, F. O. Gloeckner, D. Schüler, *Appl. Environ. Microbiol.* **2006**, *72*, 5757 – 5765.
[76] a) R. Carballido-López, *Microbiol. Mol. Biol. Rev.* **2006**, *70*, 888 – 909; b) R. M. Figge, A. V. Divakaruni, J. W. Gober, *Mol. Microbiol.* **2004**, *51*, 1321 – 1332; c) L. J. F. Jones, R. Carballido-López, J. Errington, *Cell* **2001**, *104*, 913 – 922; d) F. Van den Ent, L. A. Amos, J. Löwe, *Nature* **2001**, *413*, 39 – 44.
[77] S. Sonkaria, G. Fuentes, C. Verma, R. Narang, V. Khare, A. Fischer, D. Faivre, *PLoS One* **2012**, *7*, e34189.
[78] J. B. Rioux, N. Philippe, S. Pereira, D. Pignol, L. F. Wu, N. Ginet, *PLoS One* **2010**, *5*, e9151.
[79] N. Pradel, C. L. Santini, A. Bernadac, Y. Fukumori, L. F. Wu, *Proc. Natl. Acad. Sci. USA* **2006**, *103*, 17485 – 17489.
[80] a) E. Katzmann, A. Scheffel, M. Gruska, J. M. Plitzko, D. Schüler, *Mol. Microbiol.* **2010**, *77*, 208 – 224; b) S. Klumpp, D. Faivre, *PLoS One* **2012**, *7*, e33562.
[81] Y. Ding, J. Li, J. Liu, J. Yang, W. Jiang, J. Tian, Y. Li, Y. Pan, J. Li, *J. Bacteriol.* **2010**, *192*, 1097 – 1105.
[82] See Ref. [73a].
[83] M. A. Carillo, M. Bennet, D. Faivre, *J. Phys. Chem. B* **2013**, *117*, 14642 – 14648.
[84] O. Draper, M. E. Byrne, Z. Li, S. Keyhani, J. C. Barrozo, G. Jensen, A. Komeili, *Mol. Microbiol.* **2011**, *82*, 342 – 354.
[85] J. Baumgartner, M. A. Carillo, K. M. Eckes, P. Werner, D. Faivre, *Langmuir* **2014**, *30*, 2129 – 2136.
[86] T. Matsunaga, A. Arakaki in *Magnetoreception and magnetosomes in bacteria*, Vol. 3 (Ed.: D. Schüler), Springer, Heidelberg, **2007**, pp. 227 – 254.
[87] a) B. Yoza, A. Arakaki, T. Matsunaga, *J. Biotechnol.* **2003**, *101*, 219 – 228; b) T. Matsunaga, H. Nakayama, M. Okochi, H. Takeyama, *Biotechnol. Bioeng.* **2001**, *73*, 400 – 405; c) K. Sode, S. Kudo, T. Sakaguchi, N. Nakamura, T. Matsunaga, *Biotechnol. Tech.* **1993**, *7*, 688 – 694; d) B. Yoza, A. Arakaki, K. Maruyama, H. Takeyama, T. Matsunaga, *J. Biosci. Bioeng.* **2003**, *95*, 21 – 26.
[88] T. Matsunaga, S. Kamiya, *Appl. Microbiol. Biotechnol.* **1987**, *26*, 328 – 332.
[89] T. Tanaka, H. Yamasaki, N. Tsujimura, N. Nakamura, T. Matsunaga, *Mater. Sci. Eng. C* **1997**, *5*, 121 – 124.
[90] a) Y. Amemiya, T. Tanaka, B. Yoza, T. Matsunaga, *J. Biotechnol.* **2005**, *120*, 308 – 314; b) B. Ceyhan, P. Alhorn, C. Lang, D. Schüler, C. M. Niemeyer, *Small* **2006**, *2*, 1251 – 1255.
[91] a) See Ref. [20a]; b) M. R. Lisy, A. Hartung, C. Lang, D. Schüler, W. Richter, J. R. Reichenbach, W. A. Kaiser, I. Hilger, *Invest. Radiol.* **2007**, *42*, 235 – 241.
[92] a) T. Matsunaga, H. Togo, T. Kikuchi, T. Tanaka, *Biotechnol. Bioeng.* **2000**, *70*, 704 – 709; b) T. Matsunaga, M. Takahashi, T. Yoshino, M. Kuhara, H. Takeyama, *Biochem. Biophys. Res. Commun.* **2006**, *350*, 1019 – 1025; c) T. Yoshino, F. Kato, H. Takeyama, M. Nakai, Y. Yakabe, T. Matsunaga, *Anal. Chim. Acta* **2005**, *532*, 105 – 111.
[93] A. Roda, L. Cevenini, S. Borg, E. Michelini, M. M. Calabretta, D. Schüler, *Lab Chip* **2013**, *13*, 4881 – 4889.
[94] a) C. Lang, D. Schüler, *Appl. Environ. Microbiol.* **2008**, *74*, 4944 – 4953; b) A. Pollithy, T. Romer, C. Lang, F. D. Müller, J. Helma, H. Leonhardt, U. Rothbauer, D. Schüler, *Appl. Environ. Microbiol.* **2011**, *77*, 6165 – 6171.
[95] a) S. Martel, M. Mohammadi, O. Felfoul, Z. Lu, P. Pouponneau, *Int. J. Robot. Res.* **2009**, *28*, 571 – 582; b) S. Taherkhani, M.

Mohammadi, J. Daoud, S. Martel, M. Tabrizian, *ACS Nano* **2014**, *8*, 5049 – 5060.
[96] C. U. Herborn, N. Papanikolaou, R. Reszka, K. Grünberg, D. Schüler, J. F. Debatin, *Rofo. Fortschr. Geb. Röntgenstr. Neuen Bildgeb. Verfahr.* **2003**, *175*, 830 – 834.
[97] a) E. Alphandéry, S. Faure, O. Seksek, F. Guyot, I. Chebbi, *ACS Nano* **2011**, *5*, 6279 – 6296; b) E. Alphandéry, S. Faure, L. Raison, E. Duguet, P. A. Howse, D. A. Bazylinski, *J. Phys. Chem. C* **2011**, *115*, 18 – 22.
[98] D. Faivre, P. Agrinier, N. Menguy, P. Zuddas, K. Pachana, A. Gloter, J.-Y. Laval, F. Guyot, *Geochim. Cosmochim. Acta* **2004**, *68*, 4395 – 4403.
[99] J. Baumgartner, L. Bertinetti, M. Widdrat, A. M. Hirt, D. Faivre, *PLoS One* **2013**, *8*, e57070.
[100] J. Baumgartner, A. Dey, P. H. H. Bomans, C. Le Coadou, P. Fratzl, N. A. J. M. Sommerdijk, D. Faivre, *Nat. Mater.* **2013**, *12*, 310 – 314.
[101] a) J. C. Weaver, Q. Wang, A. Miserez, A. Tantuccio, R. Stromberg, K. N. Bozhilov, P. Maxwell, R. Nay, S. T. Heier, E. DiMasi, D. Kisailus, *Mater. Today* **2010**, *13*, 42 – 52; b) P. van der Wal, *J. Ultrastruct. Mol. Struct. Res.* **1989**, *102*, 147 – 161.
[102] P. van der Wal, H. J. Giesen, J. J. Videler, *Mater. Sci. Eng. C* **1999**, *7*, 129 – 142.
[103] J. L. Kirschvink, H. A. Lowenstam, *Earth Planet. Sci. Lett.* **1979**, *44*, 193 – 204.
[104] N. W. Runham, P. R. Thornton, D. A. Shaw, R. C. Wayte, *Z. Zellforsch. Mikrosk. Anat.* **1969**, *99*, 608 – 626.
[105] E. D. Sone, S. Weiner, L. Addadi, *J. Struct. Biol.* **2007**, *158*, 428 – 444.
[106] a) R. H. Morris, D. P. Abbott, *Intertidal invertebrates of California*, Stanford Press, Stanford, **1980**; b) "Class Polyplacophora: Morphology and Physiology": P. Kaas, A. M. Jones in *Mollusca*: *The southern synthesis part A*, *Fauna of Australia* (Eds.: P. L. Beesley, G. J. B. Ross, A. Wells), CSIRO, Melbourne, **1998**, pp. 163 – 174.
[107] P. Bouchet, J.-P. Rocroi, *Malacologia* **2005**, *47*, 1 – 2.
[108] a) N. W. Runham, *Q. J. Microsc. Sci.* **1961**, *102*, 371 – 380; b) L. A. Evans, D. J. Macey, J. Webb, *Philos. Trans. R. Soc. London Ser. B* **1990**, *329*, 87 – 96; c) K. J. Liddiard, J. G. Hockridge, D. J. Macey, J. J. Webb, W. van Bronswijk, *Molluscan Res.* **2004**, *24*, 1 – 11.
[109] L. R. Brooker, J. A. Shaw, The chiton radula: A unique model for biomineralization studies. In: *Advanced topics in biomineralization* (Ed. J. Seto) InTech **2012**.
[110] a) H. A. Lowenstam, *Science* **1967**, *156*, 1373 – 1375; b) L. R. Brooker, D. J. Macey, *Am. Malacol. Bull.* **2001**, *16*, 203 – 215; c) J. A. Shaw, D. J. Macey, P. L. Clode, L. R. Brooker, R. I. Webb, E. J. Stockdale, R. M. Binks, *Am. Malacol. Bull.* **2008**, *25*, 35 – 41; d) M. Saunders, C. Kong, J. A. Shaw, P. L. Clode, *Micorsc. Microanal.* **2011**, *17*, 220 – 225.
[111] a) K. M. Towe, H. A. Lowenstam, *J. Ultrastruct. Res.* **1967**, *17*, 1 – 13; b) K. S. Kim, D. J. Macey, J. Webb, S. Mann, *Proc. R. Soc. London Ser. B* **1989**, *237*, 335 – 346; c) "Structure and formation of the magnetite-bearing cap of the polyplacophoran tricuspid radula teeth": P. van der Wal in *Iron Biominerals* (Eds.: R. B. Frankel, R. P. Blakemore), Plenum, New York, **1990**, pp. 221 – 229.
[112] a) L. R. Brooker, A. P. Lee, D. J. Macey, W. van Bronswijk, J. Webb, *Mar. Biol.* **2003**, *142*, 447 – 454; b) A. P. Lee, L. R. Brooker, D. J. Macey, J. Webb, W. van Bronswijk, *J. Biol. Inorg. Chem.* **2003**, *8*, 256 – 262; c) M. Saunders, C. Kong, J. A. Shaw, D. J. Macey, P. L. Clode, *J. Struct. Biol.* **2009**, *167*, 55 – 61; d) L. A. Evans, D. J. Macey, J. Webb, *Acta Zool.* **1994**, *75*, 75 – 79; e) L. R. Brooker, A. P. Lee, D. J. Macey, J. Webb, W. van Bronswijk, *Venus* **2006**, *65*, 71 – 80.
[113] A. P. Lee, L. R. Brooker, W. Van Bronswijk, D. J. Macey, J. Webb, *Biopolymers* **2003**, *72*, 299 – 301.
[114] a) H. A. Lowenstam, *Chem. Geol.* **1972**, *9*, 153 – 166; b) D. J. Macey, J. Webb, L. R. Brooker, *Bull. Inst. Oceanogr.* **1994**, *4*, 191 – 197.
[115] A. P. Lee, L. R. Brooker, D. J. Macey, W. van Bronswijk, J. Webb, *Calcif. Tissue Int.* **2000**, *67*, 408 – 415.
[116] Q. Wang, M. Nemoto, D. Li, J. C. Weaver, B. Weden, J. Stegemeier, K. N. Bozhilov, L. R. Wood, G. W. Milliron, C. S. Kim, D. Kisailus, *Adv. Funct. Mater.* **2013**, *23*, 2908 – 2917.
[117] L. K. Grunenfelder, E. Escobar de Obaldia, Q. Wang, D. Li, B. Weden, C. Salinas, R. Wuhrer, P. Zavattieri, D. Kisailus, *Adv. Funct. Mater.* **2014**, *24*, 6093 – 6104.
[118] J. C. Weaver, G. W. Milliron, A. Miserez, K. Evans-Lutterodt, S. Herrera, I. Gallana, W. J. Mershon, B. Swanson, P. Zavattieri, E. DiMasi, D. Kisailus, *Science* **2012**, *336*, 1275 – 1280.
[119] R. J. Wealthall, L. R. Brooker, D. J. Macey, B. J. Griffin, *J. Morphol.* **2005**, *265*, 165 – 175.
[120] L. A. Evans, D. J. Macey, J. Webb, *Mar. Biol.* **1991**, *109*, 281 – 286.
[121] a) C. M. Hansel, S. G. Benner, S. Fendorf, *Environ. Sci. Technol.* **2005**, *39*, 7147 – 7153; b) Y. Noguchi, T. Fijiwara, K. Yoshimatsu, Y. Fukomori, *J. Bacteriol.* **1999**, *181*, 2142 – 2147.
[122] H. J. Choi, S. W. Kang, C. . Yang, S. G. Rhee, S. E. Ryu, *Nat. Struct. Biol.* **1998**, *5*, 400 – 406.
[123] M. Nemoto, Q. Wang, D. Li, S. Pan, T. Matsunaga, D. Kisailus, *Proteomics* **2012**, *12*, 2890 – 2894.
[124] L. M. Gordon, D. Joester, *Nature* **2011**, *469*, 194 – 198.
[125] a) E. I. Jones, R. A. McCance, L. R. B. Shackleton, *J. Exp. Biol.* **1934**, *12*, 59 – 64; b) S. Mann, C. C. Perry, J. Webb, B. Luke, R. J. P. Williams, *Proc. R. Soc. London Ser. B* **1986**, *227*, 179 – 190.
[126] M. A. Burford, D. J. Macey, J. Webb, *Comp. Biochem. Physiol. Part A* **1986**, *83*, 353 – 358.
[127] E. D. Sone, S. Weiner, L. Addadi, *Cryst. Growth Des.* **2005**, *5*, 2131 – 2138.
[128] H.-K. Lu, C.-M. Huang, C.-W. Li, *Exp. Cell Res.* **1995**, *219*, 137 – 145.
[129] a) H. Ehrlich, P. Simon, W. Carrillo-Cabrera, et al., *Chem. Mater.* **2010**, *22*, 1462 – 1471; b) C. Lüter in *Brachipods-past and present* (Eds.: C. H. C. Brunton, L. R. M. Cocks, S. L. Long), Taylor & Francis, London, **2001**; c) C. Lüter, *Proc. R. Soc. London Ser. B* **2004**, *271*, S465 – S467; d) C. B. Miller, D. M. Nelson, C. Weiss, A. H. Soeldner, *Mar. Biol.* **1990**, *106*, 91 – 101.
[130] a) G. W. Grime, F. Watt, S. Mann, C. C. Perry, J. Webb, R. J. P. Williams, *Trends Biochem. Sci.* **1985**, *10*, 6 – 10; b) S. Mann, J. Webb, R. J. P. Williams, *Biomineralization*: *Chemical and Biochemical Perspectives*, Wiley-VCH, Weinheim, **1989**.
[131] K. J. Liddiard, J. G. Hockridge, D. J. Macey, J. J. Webb, W. van Bronswijk, *Molluscan Res.* **2004**, *24*, 1 – 11.
[132] H. A. Lowenstam, *Science* **1981**, *171*, 487 – 490.
[133] T. G. St Pierre, S. Mann, J. Webb, D. P. E. Dickson, N. W. Runham, R. J. P. Williams, *Proc. R. Soc. London Ser. B* **1986**, *228*, 31 – 42.
[134] See Ref. [110a].
[135] a) J. M. McBride, S. B. Bertman, *Angew. Chem. Int. Ed. Engl.* **1989**, *28*, 330 – 333; *Angew. Chem.* **1989**, *101*, 342 – 344; b) I. Weissbuch, L. Addadi, M. Lahav, *Science* **1991**, *253*, 637 – 645; c) B. Kahr, J. M. McBride, *Angew. Chem. Int. Ed. Engl.* **1992**, *31*, 1 – 26; *Angew. Chem.* **1992**, *104*, 1 – 28.
[136] a) M. Kosmulski, S. Durand-Vidal, E. Maczka, J. B. Rosenholm, *J. Colloid Interface Sci.* **2004**, *271*, 261 – 269; b) U. Schwertmann, R. M. Cornell, *Iron Oxides in the laboratory*: *Preparation and characterization*, *2nd ed.*, Wiley-VCH, Weinheim, **2000**.
[137] a) R. M. Taylor, U. Schwertmann, *Clays Clay Miner.* **1978**, *26*, 373 – 383; b) J. Cumplido, V. Barron, J. Torrent, *Clays Clay Miner.* **2000**, *48*, 503 – 510.

[138] J. Detournay, M. Ghodsi, R. Derie, *Z. Anorg. Allg. Chem.* **1975**, *412*, 184 – 192.
[139] T. G. Quinn, G. J. Long, C. G. Benson, S. Mann, R. J. P. Williams, *Clays Clay Miner.* **1988**, *36*, 165 – 175.
[140] K. Thorstensen, I. Romslo, *Biochem. J.* **1990**, *271*, 1 – 10.
[141] K. Eusterhues, F. E. Wagner, W. Hausler, M. Hanzlik, H. Knicker, K. U. Totsche, I. Kogel-Knabner, U. Schwertmann, *Environ. Sci. Technol.* **2008**, *42*, 7891 – 7897.
[142] G. Krishnamurti, P. Huang, *Clays Clay Miner.* **1991**, *39*, 28 – 34.
[143] A. Navrotsky, L. Mazeina, J. Majzlan, *Science* **2008**, *319*, 1635 – 1638.
[144] G. W. Scherer, *Cement Concrete Res.* **1999**, *29*, 1347 – 1358.
[145] K. Yu, T. Fan, S. Lou, D. Zhang, *Prog. Mater. Sci.* **2013**, *58*, 825 – 873.
[146] C. T. Lefevre, D. Trubitsyn, F. Abreu, S. Kolinko, C. Jogler, L. G. P. de Almeida, A. T. R. de Vasconcelos, M. Kube, R. Reinhardt, U. Lins, D. Pignol, D. Schüler, D. A. Bazylinski, N. Ginet, *Environ. Microbiol.* **2013**, *15*, 2712 – 2735.

Received: September 8, 2014

